TRANSIENTS IN A MONOTUBE BOILER

--A DIGITAL SIMULATION

by

Arthur Wilfred Gardiner

Thesis submitted to the Graduate Faculty of the

Virginia Polytechnic Institute and State University

in partial fulfillment of the requirements for the degree of

DOCTOR OF PHILOSOPHY

in

Mechanical Engineering

APPROVED:

F. J. Pierce, Chairman

J. B. Jones

W. C. Thomas

H. L. Wood

H. G. Campbell

March, 1973

Blacksburg, Virginia

ACKNOWLEDGMENTS

It is a pleasure to recognize the people who have aided me in this scholastic endeavor. To my major adviser, Dr. F. J. Pierce, I am grateful for advice and discussion on subjects academic and otherwise, in addition to criticisms as required. I taught for Dr. J. B. Jones who went beyond the call of duty in regard to financial support and teaching assignments. Dr. W. C. Thomas taught me heat transfer both in and out of class and kept the computer running. Dr. H. L. Wood helped me on the sophisticated instrumentation he knows so well--but we did not have time to utilize fully. Professor H. G. Campbell taught me linear algebra and tried to keep my mathematics on the straight and narrow.

I also owe a vote of thanks to Shorty and the men in the shop who made the apparatus, and to H. D. Garner of NASA-Langley for his encouragement and information on the latest literature.

Finally, my endless thanks to my partner Nancy who kept the chin up and home fires burning during these lean years.

TABLE OF CONTENTS

TABLE OF CONTENTS - continued

LIST OF FIGURES

LIST OF FIGURES - continued

SYMBOLS

A	area
a	a constant
A/F	air-fuel ratio (mass basis)
b	a constant
BC	boundary condition(s)
BTE	brake thermal efficiency
c	a constant
c_p	specific heat
D	coil diameter of curvature
d	inside tube diameter
d_o	outside tube diameter
e	specific stored energy
F	length fraction of tube segment at which saturation occurs
FDE	finite difference equation(s)
G	mass flux = mass flow rate ÷ minimum flow area
H	total enthalpy
h	specific enthalpy
HV	heating value
ICE	internal combustion engine
ICP	Ideal Cylinder Performance (program)
k	thermal conductivity
ℓ	length of tube segment
LHS	left hand side

SYMBOLS - continued

m	mass flow rate
n	number of coils
ODE	ordinary differential equation(s)
p	pressure
PBO	steam pressure at boiler outlet
PDE	partial differential equation(s)
PEP	predicted engine performance (program)
Pr	Prandtl Number
PSC	steam chest (maximum) pressure
Q	total heat flow rate
q	heat flux
QLOSSF	fraction of fuel HV lost to ambient
R	gas constant; average relative change of v and h during one time step
r	tube radius
RCA	Rankine cycle analysis (program)
RCE	rankine cycle efficiency
Re	Reynolds number
RHS	right hand side
s	tube spacing
SBP	Steady Boiler Performance (program)
T	temperature
t	time
TAMB	ambient air temperature

SYMBOLS - continued

TBO	steam temperature at boiler outlet
TBP	Transient Boiler Performance (program)
TCOND	condenser temperature
TSECON	steam temperature at economizer inlet
TSC	steam chest (maximum) temperature
V	total volume
v	specific volume
VR	volumetric expansion ratio
WDG	gas flow rate
WDS	steam flow rate
x	distance along tube axis; steam quality
y	convective heat transfer coefficient

Greek Letters

α	thermal diffusivity
η	efficiency
μ	absolute viscosity
ρ	density
τ_0	wall shear stress

Subscripts

ad	adiabatic
amb	ambient
b	boiler
c	condenser

SYMBOLS - continued

cc	combustion chamber
e	engine
f	fuel; friction
fl	flue
g	gas
i	steam side station index
L	loss to ambient
ℓ	liquid
m	gas side station index
o	outside; out
r	radiation
s	steam
t	tube; total; transverse
v	vapor
2ph	two phase

Superscripts

$\bar{x}$	bar signifies average value of x
'(prime)	new time point

I. INTRODUCTION

1.1. Motivation

Air pollution is now recognized as a serious national problem. A major portion of this pollution is attributed to motor vehicles. So important is this problem that it has precipitated a series of state and federal regulations governing the maximum allowable level of pollutants in automotive exhausts. To date, these laws have been satisfied through modifications of the conventional internal combustion engine (ICE). However, as the regulations become more stringent, these modifications will become more costly and troublesome. As a result of this pressure, engine manufacturers and government agencies are investigating alternative powerplants. One of the more promising of these is based on the Rankine or vapor cycle and is popularly called a steam engine (1,2).* To be an acceptable replacement for the highly developed ICE in the modern car, a steam engine must be compact, safe, and agile as well as non-polluting. The size and responsiveness of a complete steam powerplant is primarily a function of the type of steam generator (boiler) employed. A once-through monotube boiler optimizes these characteristics.

A monotube boiler consists of a single tube wound into a series of spiral coils. Combustion gases pass around the tubing in this stack of coils to the flue. Feed-water is pumped into the flue end of the

---

* Numbers in parentheses refer to references on page 72.

tube and finally emerges from the combustion chamber end as superheated steam. Thus there is no circulation since the water passes through the tube only once before going to the engine. This type of boiler has a large ratio of heat transfer area to water volume, which leads to fast response. The small mass of fluid contained contributes to greater safety in case of tube failures. However, these advantages are accompanied by several penalties. The small inventory of heated water means that an increase in demand for steam can quickly empty the boiler unless a fast-reacting control system immediately pumps in more feedwater and fuel. The resulting hesitation when one "steps on the gas" is definitely disconcerting and even dangerous. On the other hand if the control pumps in too much water and fuel, the steam pressure and temperature may exceed safe limits which leads to tube failure and/or excessive engine wear. Thus, even the most elementary control must closely regulate outlet steam temperature and pressure, despite fluctuating demand, through judicious variation in inlet water and fuel rates. But for the most rapid possible response, it is likely that water will be injected and temperature/pressure measured at several points along the tube. With this large number of variables to be considered, it would be wasteful to adopt a purely cut-and-try approach to the development of an optimum control system. To expedite this work, a mathematical model of the boiler should be employed. This transient model could then be used to analytically test candidate control strategies under a range of simulated operating conditions. In this manner the more promising control algorithms may be identified and

then receive the detailed attention they deserve. Thus, there appears to be a current need for a simulation of a monotube boiler under transient conditions.

1.2. Plan of Attack

The boiler is a system whose dependent variables are the outlet steam pressure and temperature. Both these properties must be maintained within narrow limits despite the random disturbance to the exit steam flow rate provided by the driver's throttle foot responding to the traffic situation. To meet these conditions the engineer must control the independent variables water rate and firing rate. Therefore, to be useful in control system analysis the boiler simulation should provide for changes in these variables. The present research is designed to be the engineering tool needed for this control work.

To provide this tool several steps must be taken. First, the mathematical relationships which describe the physical situation must be assembled. Since a boiler is basically a fluid flow device, our general relations will be the conservation laws for mass, momentum and energy. These will be augmented with phenomenological equations for heat transfer and pressure drop. The equations of state relating the thermodynamic variables will complete the mathematical model. The second step is the development of a method of solving the equations to get numbers on a digital computer. When put in finite difference form for numerical solution, the general relations constitute a matrix equation with a variable coefficient matrix. To solve this set of

equations consideration will be given to purely iterative methods, the solution of each equation separately plus iteration, and a truly simultaneous solution. The simultaneous solution represents the real situation best but is more difficult from a computational standpoint.

When the simulation is operating, its predictions will be compared with results reported in the literature and preliminary test results from an automotive-size boiler which has been built.

1.3. Preliminary Studies

This simulation is as flexible as appeared feasible but any specialization which was needed was always made in favor of an automotive boiler. Some of these decisions will be discussed along with the reasons behind them.

The choice of an optimum working fluid for a Rankine powerplant has received much attention (3,4,5). Water has the disadvantages of high freezing point, poor shape of the saturation dome on a temperature-entropy diagram and high enthalpy change per pound when expanded. The latter weakness leads to a large volumetric expansion ratio in an engine, or many stages in a turbine, either of which make the powerplant more complex. However, alternate fluids have weaknesses such as high cost, toxicity and chemical instability at the high temperatures (800-1200 F) that an efficient powerplant must use. In fact, some fluids suffer an excessive pressure drop across the valves at reasonable engine speeds (6). From the above it is clear that the ideal fluid has not been found. This research used water since the resulting

mathematical model can be extended to another fluid rather easily if desired.

The choice of nominal steam temperatures and pressure is a compromise. It is well known that high values increase thermal efficiency (7,8). However, very high pressures shorten piston ring life, increase boiler weight and require huge expansion ratios to realize the efficiency potential. If a turbine is being contemplated, high pressure reduces the turbine size for a given power, thereby increasing the already serious problems of low turbine efficiency and multistage reduction gearing. Very high temperature increases material problems in superheater, valves and pistons but it does give a significant improvement in thermal efficiency with no increase in volume expansion ratio. To ascertain optimum steam conditions parametric studies have been made of the Rankine cycle using a Rankine Cycle Analysis (RCA) computer program. A Rankine cycle is a simple cycle involving only a boiler feed pump, steam generator, engine or turbine and condenser. In some nineteenth century texts it is considered a saturated steam cycle but this definition has been relaxed in recent years to include superheated steam. A Rankine cycle does not include any reheat or regeneration and assumes ideal processes, e.g., no pressure drop in the boiler or condenser and complete isentropic expansion to the exhaust pressure within the cylinder. RCA computes Rankine cycle parameters directly from steam table data found in the STEAMT subroutine listed in Appendix E. It is fast (several hundred cases per minute) and therefore useful for making a wide-ranging survey of simple steam

powerplant cycles. From RCA data we plot Fig. 1.1 which shows the effect of volume expansion ratio, VR, on cycle efficiency, RCE, for various steam chest temperatures, TSC, and pressures, PSC. For constant TSC, increasing PSC requires large increases in VR for only a small increase in RCE. However, at constant PSC, an increase in TSC permits a reduction in VR with a large increase in efficiency. Thus a high maximum temperature is a prime requirement for high realizable thermal efficiency. A temperature of only 800 F has been chosen for this research solely to avoid boiler tube problems in the early (more uncertain) phases of the experimental work.

The next step in the direction of reality in the simulation of the engine (expander) only is provided by the Ideal Cylinder Performance (ICP) program. This adds the effect of clearance volume, admission valve closing point (cutoff) and exhaust valve closing (compression). The isentropic exponent ($\gamma = c_p/c_c$) is computed from STEAMT and used to compute the work of the idealized indicator diagram. Thus ICP includes the effect of incomplete expansion on the power stroke of the piston and free expansion of the fresh steam at the end of the compression stroke. From the resulting indicated values, a friction mean effective pressure is subtracted to give an approximation of the brake performance. ICP is well suited to a study of the effect of condenser performance on the power plant.

Figure 1.2 shows the effect of condenser temperature, TCOND, on brake thermal efficiency, BTE, for various PSC. As expected, BTE increases with decreasing TCOND so a low TCOND is desirable. However,

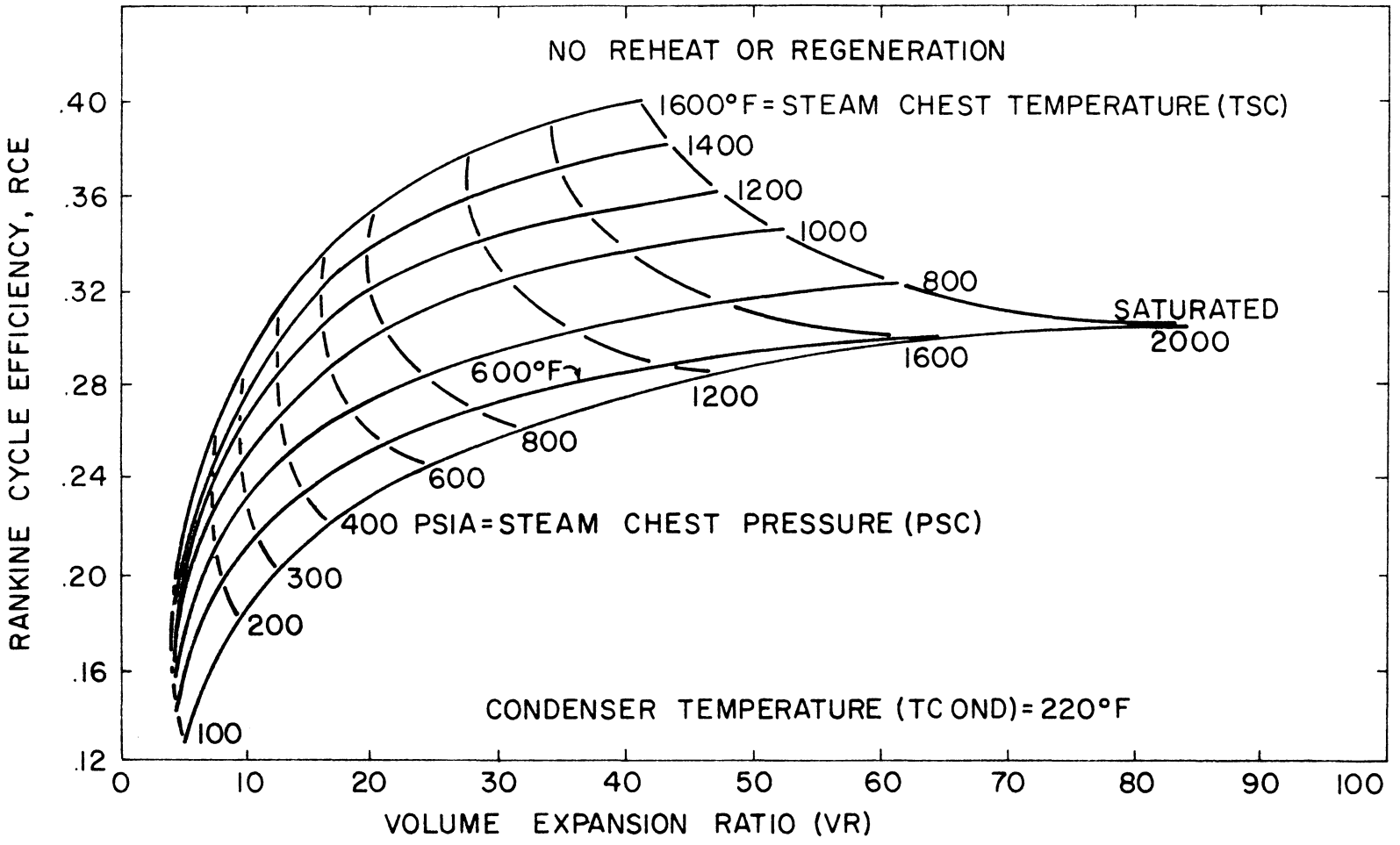

FIG. 1.1 EFFECT OF EXPANSION RATIO ON RANKINE CYCLE EFFICIENCY FOR VARIOUS STEAM CHEST TEMPERATURES AND PRESSURES

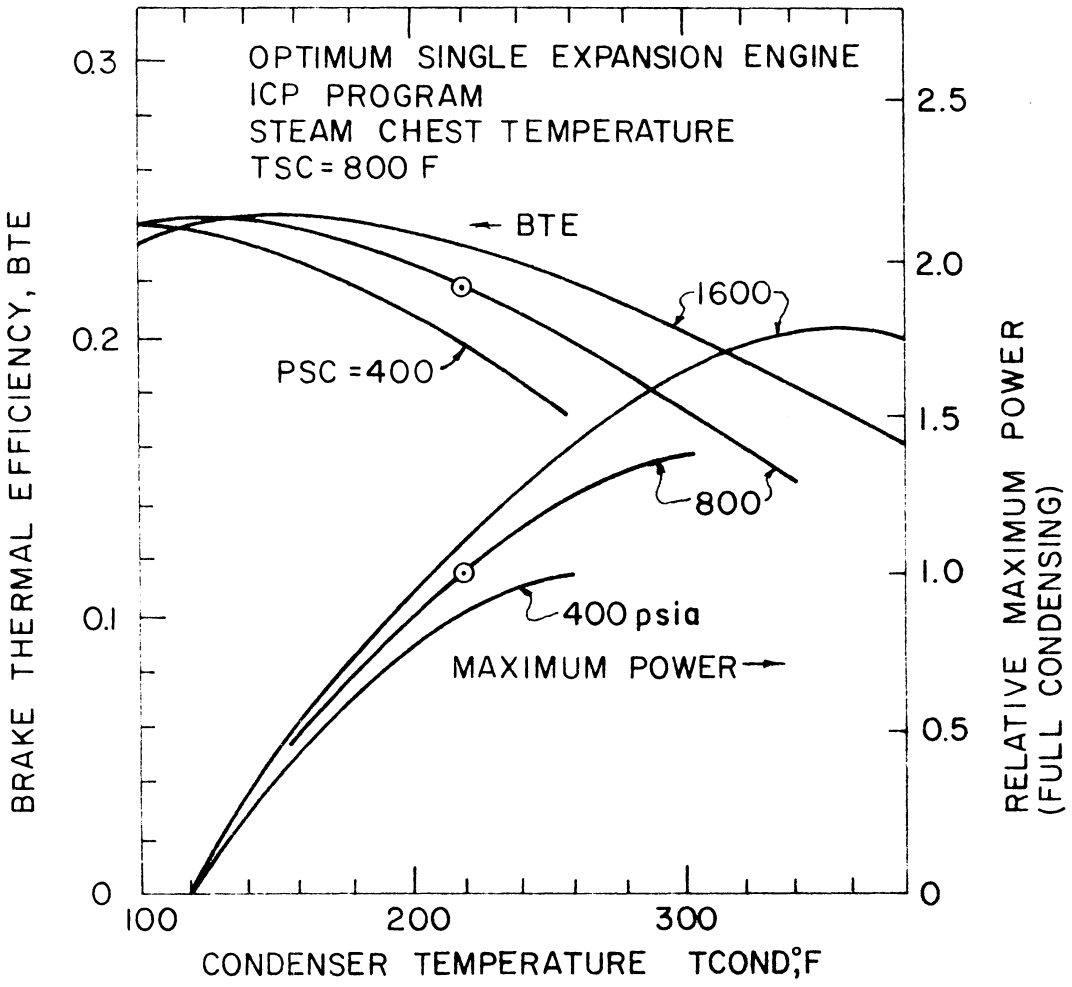

FIG. I.2 THE EFFECT OF CONDENSER TEMPERATURE ON BRAKE THERMAL EFFICIENCY AND MAXIMUM RELATIVE POWER FOR VARIOUS STEAM CHEST PRESSURES.

any practical steam car must condense essentially all its water, so for a given condenser size the maximum engine power depends on engine efficiency and temperature difference between steam and air. (See Appendix A). The combined effect of these two variables is demonstrated by the second set of curves in Fig. 1.2 which shows that for maximum power with full condensing a high TCOND is desirable. In other words, we cannot obtain high efficiency and power at the same time. This classic compromise between efficiency and condenser size is more difficult for the air-cooled condenser in an automotive application.

A third engine simulation models the details of actual valve-opening diagrams, pressure drop through the valves, leakage, heat transfer in the cylinder, and the variation of mechanical friction with load and speed. It integrates differential equations for mass flow through admission and exhaust valves, cylinder pressure, and mean effective pressure around the engine cycle. This program is sufficiently complete to give the actual Predicted Engine Performance (PEP). The basic general conclusion from this PEP program is that the ICP program gives a good prediction of efficiency but a high power since it does not include pressure drop through the valves.

The three programs mentioned above are not described herein since they are not the subject of this research. However, their use provided data from which it is concluded that the chosen values of 800 psi, 800 F and 220 F are realistic steam conditions and feedwater temperature for steam automobiles.

II. LITERATURE REVIEW

Before discussing previous work in the area of boiler simulation it appears prudent to define the two basic types of boilers. The water-level type is characterized by a large drum in which a water level is maintained at a constant position. Water moves through a large number of short parallel tubes by natural circulation. While in passage through these heated tubes some of the water evaporates. This steam is separated from the liquid and then passes from the drum to the superheater tubes.

On the other hand, a monotube boiler does not have a fixed water level. Feed water is pumped into one end of a heated tube and gradually evaporates as it moves through the tube until eventually all the droplets of liquid water have disappeared. This point, which corresponds to the saturated vapor line, moves back and forth in the tube as the steam rate changes, so a monotube does not have a fixed water level. As a result of its forced circulation the monotube also escapes the numerous limitations on layout which natural circulation places on the water level type.

These essential differences indicate that the analytical model of a water level boiler would be of only limited utility in a monotube simulation. This fact excludes some boiler literature from extensive review.

2.1. Control Systems

Current work on the control of fast response automotive steam generators can be best appreciated against a background of the classical work in this area. The Stanley used a water-level boiler. This level was closely regulated through control of the boiler feed pump. Steam pressure controlled the firing rate. This system is simple, reliable, and has a large steam reserve. However it is also heavy and slow to attain maximum output when started from cold. A qualitative review of monotube boiler control systems has been given by Doble (9). The Serpollet monotube employed an auxiliary engine which drove all the pumps, thereby assuring a fixed ratio of fuel to water flow. This system was too inflexible since it could not handle abnormal situations. The White monotube used a system which sensed water flow rate in addition to steam outlet temperature and pressure. This was probably the best of the early (pre 1910) controls. Doble has developed two techniques. The first uses a "normalizer" which injects a portion of the feedwater into the superheater portion of the tubing to control over-temperature. The second uses a "triple-effect" thermostat which responds to the average of feedwater, saturation and outlet temperatures. McCulloch (10) employed a combination of Doble's methods. No evidence has been found of the use of a mathematical model of boiler transients by these early experimenters.

The best current review of control systems for steam automobiles is provided by Garner (11). His review is purely qualitative, again due to the absence of applicable simulations in the area. In fact he

concludes another of his articles (12) by stating, "... perhaps the most valuable bit of research which could be implemented for the advancement of steam car engineering would be the development of the generalized transfer functions of the automotive monotube boiler, and the relation of their various coefficients to the physical parameters of the specific boiler."

2.2. Peripheral Work

Until recently, most modern research on small Rankine cycle powerplants was directed toward military or space applications (13,14). Many of these prime movers drive electrical alternators at constant speed (15) while others are further simplified by forcing them to deliver constant power (16,17). Others are part of a compound system (18) which is probably too complex for automotive use. Modern Rankine engines intended specifically for automobiles usually rely on the same control concepts employed by the classical steamers. The General Motors SE-101 (19) senses steam temperature and pressure at one point in order to control three-step water and fuel pumps and a normalizer. Some writers on control systems simplify the problems by eliminating vital elements like the superheater (20). But superheat is important since it improves the ideal cycle efficiency without increase in volume expansion ratio while eliminating the cylinder condensation which occurs in a real engine. Other workers introduce problems that will not concern a steam car. For example, the assumption of a constant pressure feed pump leads to "static" or

"pressure drop" instability (21). This occurs when the boiler is operated in a state such that an increase in water flow rate causes a decrease in pressure drop. This leads to an increased flow rate, etc. so an unstable situation exists. However an automotive steam plant will employ a positive displacement pump which delivers a constant flow rate (at a given speed) regardless of pressure. If the feed pressure is pulsed, however, instabilities can develop at certain frequencies (22). The monotube boiler can suffer from other types of instability (22,23,24). An acoustic disturbance may cause mechanical vibration but it is usually random and does not couple with other boiler components. Though much of this work is not useful relative to the problem at hand, it does serve as a reminder that several types of flow instabilities exist in monotube boilers. However, no record has been uncovered indicating that they have caused trouble in steam car boilers.

2.3. Modern Research

In the more applicable modern work, Peoples (25) assumes a first order time lag between the change in fuel rate and the resulting change in steam rate. As will be shown, this is a reasonable approximation if a pure, or transport, lag is also included. He does not give any method for calculating the time constant of the system.

Richards and Garner (26) have written a simulation which assumes constant pressure in a boiler having preheating, evaporation and superheating sections. All heat transfer and transport properties are assumed constant for a given section. The entire counterflow boiler

consists of 120 segments with an explicit energy balance equation for each. The prime limitations here are the lumping of all tube wall temperatures into one per segment and the assumption of constant density in the two-phase region. The latter removes the problem of using steam tables but is a major weakness at the pressure (800 psi) considered here since the density ratio (and hence velocity ratio) between saturated liquid and vapor is 27 for the nominal steam conditions used. Buis (27) has developed a hybrid (analog and digital) simulation for the purpose of studying the pressure waves in boilers. These high frequency waves are more difficult to reproduce accurately than the low frequency thermal waves of interest here. The characteristics of the hyperbolic equations must be calculated and the direction of integration varied to suit these characteristics. This approach appears to be fast and accurate and deserves further consideration but its implementation does require an extensive hybrid computer facility.

In recent years the Environmental Protection Agency (EPA) has sponsored research in steam car design. One of their contracts to provide a complete automotive steam powerplant was let to Steam Engine Systems Corporation who in turn subcontracted with Bendix Corporation for the control system. Bendix (28) has also developed a hybrid simulation though it includes not only the boiler but the control system, engine and vehicle. The boiler is broken into preheater, evaporator and superheater sections of constant length. A simple polynomial curve fit plus the Clapeyron equation were used for an equation of state. Though the simulation is claimed to represent a particular boiler well,

the simplifications above limit it to the study of existing boilers, i.e., it is dependent upon numerous experimental coefficients. No experimental results are given.

In the last 20 years the once-through boiler has become more popular in central power stations. Adams, et al. (29) have linearized the general equations and converted them to a set of ordinary differential equations (ODE) through lumping. In this technique the three PDE which govern the entire boiler are replaced by a set of three ODE in time for each section of the boiler. The dependent variables are averages or lumped values which hold for the entire section. This lumping permits an analog simulation but 160 amplifiers are required and due to the linearizations only small perturbations may be studied. This paper gives some transients for a 1.3 million lbm steam/hr boiler-turbine but the description of the plant is inadequate for a test run on the simulation described in this research. Livshits, et al. (30) have reported the transient response of a 250 metric ton/hr (about 550,000 lbm/hr) boiler. Though no simulation or boiler details are given it is interesting to note that for a minimum change in tube temperature the water rate was increased 30 sec. after the fuel rate was raised.

The frequency response of monotube boilers have been studied by NASA-Lewis and their contractors. Krejsa and co-workers (31) have boiled freon in a water heated counterflow boiler in which the freon feed rate was varied sinusoidally at frequencies of 0.04-4.0 cps. The exit quality was limited to 12-63%.

Hess and collaborators (23) report extensive results of tests on a water heated boiler using counter flowing water as the working fluid. Steady state, step response and frequency response tests were performed in a search for a model to predict instabilities. These workers report a non-equilibrium condition can exist at the boiler exit in which superheated steam and saturated water droplets co-exist. This violates the underlying premise of classical thermodynamics and introduces a most undesirable new variable to be determined. Though this is not a combustion heated boiler the results will be qualitatively compared with those reported here in the Results section.

From this literature review one concludes that a detailed all-digital simulation has not been attempted and no transient results are available for a fully described, combustion-heated, monotube boiler.

III. MATHEMATICAL MODEL

3.1. Definitions and Assumptions

In this work we define the mathematical model as the set of equations which are used to describe the physical situation of interest. A simulation is a broader term which includes the mathematical model, the method of solving the equations, and the detailed programming of the computer.

Before introducing the basic equations the assumptions should be discussed. Fundamental to the entire analysis is the assumption of one-dimensional flow. This implies the absence of gradients of any kind in the radial and circumferential directions. The fact that radial temperature and velocity gradients actually do exist is accounted for through empirical relations for heat transfer and pressure drop which are modified to account for the curvature of the coiled tube. Both radiation and convection heat flux will vary around the tube periphery but only average values are used here. The variation in tube diameter from coil to coil is provided for through a variation in velocity which is inversely proportional to the variation in flow area.

Energy storage in the casing is ignored, though provision is made for the heat loss to ambient. Energy storage in the gas is also neglected--it is assumed that the energy release rate of the fire can be changed instantaneously. This is taken to be a problem in classical thermodynamics, i.e., equilibrium exists to permit valid use of average

properties.

3.2. General Laws

The general laws applicable here are the conservation laws of mass, momentum and energy in their one-dimensional form. We derive these in integral form for a control volume with fluid entering at station i and leaving at i+1. The conservation of mass may be written:

rate of mass increase in volume = net mass flow in across boundary

$$\frac{d}{dt}\int \rho dV = \rho u A_i - \rho u A_{i+1} \tag{3.1}$$

Newton's Second Law of Motion, or the momentum equation, is:

rate of momentum increase in volume + net momentum flow out = net normal force + net shear force

$$\frac{d}{dt}\int \rho u dV + \rho u^2 A_{i+1} - \rho u^2 A_i = pA_i - pA_{i+1} - \Delta p_{friction} A_i \tag{3.2}$$

The First Law of Thermodynamics or the energy equation may be written:

rate of increase of energy in volume = net rate of energy convected in − rate of stress work on boundary + heat flow rate in

$$\frac{d}{dt}\int \rho e dV = \rho u A e_i - \rho u A e_{i+1} + pAu_i - pAu_{i+1} + \Delta p_{friction}\, \bar{u} A_i + Q \tag{3.3}$$

These general laws are written above in what is called the "conservation form" since the quantities being conserved, namely mass, ρ, momentum, ρu, and stored energy, ρe, per unit volume, all appear explicitly. Within the limitations of the assumptions these equations are exact even in finite difference form if the integral can be accurately evaluated.

The differential form of these equations can be derived from the integral form by differentiating the integral, dividing through by $\Delta V = A\Delta x$, and going to the limit $\Delta x \to 0$:

$$\frac{\partial \rho}{\partial t} + \frac{\partial \rho u}{\partial x} = 0 \tag{3.4}$$

$$\frac{\partial \rho u}{\partial t} + \frac{\partial \rho u^2}{\partial x} + \frac{\partial p}{\partial x} = \frac{\partial p_f}{\partial x} \tag{3.5}$$

$$\frac{\partial \rho e}{\partial t} + \frac{\partial \rho u e}{\partial x} + \frac{\partial p u}{\partial x} = \frac{dQ}{dV} - u \frac{\partial p_f}{\partial x} \tag{3.6}$$

These equations are still in conservation form. To permit easy use of the steam tables the variables enthalpy, h, and specific volume, v, are introduced. The stored energy is

$$e = h - pv + \frac{u^2}{2}$$

and

$$\rho = \frac{1}{v}$$

so the equations become

$$\frac{\partial v}{\partial t} + u \frac{\partial v}{\partial x} - v \frac{\partial u}{\partial x} = 0 \tag{3.7}$$

$$\frac{\partial u}{\partial t} + u \frac{\partial u}{\partial x} + v \frac{\partial p}{\partial x} = v \frac{\partial p_f}{\partial x} \tag{3.8}$$

$$\frac{\partial h}{\partial t} + u \frac{\partial h}{\partial x} + u \frac{\partial u}{\partial t} + u^2 \frac{\partial u}{\partial x} - v \frac{\partial p}{\partial t} = v \frac{Q}{V} - v\, u \frac{\partial p_f}{\partial x} \tag{3.9}$$

Most of this research effort has been devoted to solving the general laws in this form.

3.3. Equations of State

Several particular laws are needed to complete the mathematical model of the system. The thermodynamic properties are related by equations of state, i.e., by steam table data:

$$v = f(T,p) \quad \text{or} \quad v = f(T,x) \tag{3.10}$$

and

$$h = f(T,p) \quad \text{or} \quad h = f(T,x) \tag{3.11}$$

where here x is steam quality and h is enthalpy.

These relations, plus transport properties, are available in a subroutine STEAMT and are discussed in Appendix C.

3.4. Steam-side Convection Coefficient and Pressure Drop

In this research we rely entirely on empirical data--no effort is made to determine these data from first principles. Since the heat transfer to the steam is required we must determine the convection

coefficients h_ℓ and h_v. For the fully developed turbulent flow of liquid water in straight circular tubes, Kays (32) recommends

$$\frac{h_\ell d}{k} = 0.155\ Re^{0.83}\ Pr^{0.5} \tag{3.12}$$

while for gases in the same flow situation he suggests

$$\frac{h_v d}{k} = 0.021\ Re^{0.8}\ Pr^{0.6} \tag{3.13}$$

The pressure drop is

$$\Delta p_f = \tau_0 \frac{4\ell}{d} \tag{3.14}$$

where the shear stress

$$\tau_0 = f \frac{G^2}{2\rho} \tag{3.15}$$

depends on the friction factor (32)

$$f = 0.046\ Re^{-0.2} \tag{3.16}$$

For curved tubes a secondary flow develops which increases both the friction factor and the heat transfer coefficient by a factor (32)

$$[Re\ (\frac{d}{D})^2]^{0.05} \tag{3.17}$$

where d is the tube diameter and D the coil diameter of curvature.

Combining the above we get

$$h_\ell = 0.155\ (\frac{d}{D})^{0.1} \frac{k}{d} Re^{0.88}\ Pr^{0.5} \tag{3.18}$$

$$h_v = 0.021 \left(\frac{d}{D}\right)^{0.1} \frac{k}{d} Re^{0.85} Pr^{0.6} \tag{3.19}$$

$$\Delta p_f = 0.184 \left(\frac{d}{D}\right)^{0.1} Re^{-0.15} \tag{3.20}$$

These relations pertain to single-phase flow. For the two-phase flow in the evaporation zone the physical situation is far more complex. Despite a large mass of literature on the subject (33,34) no single relation which covers the entire range of steam quality has been found. However, Peterson (35) has presented a design procedure based on piecing together existing correlations. He shows that in general, heat transfer and pressure drop increase in the two-phase region. With this fact as a point of departure, the relations used herein are original to this investigation and are based on a linear combination of liquid and vapor coefficients multiplied by a two-phase factor. The final equations, given below, are in general agreement with the literature in this area:

$$h_{2ph} = [xh_v + (1 - x)h_\ell][1.5 - 0.5 \cos (2\pi x)]$$

$$\Delta p_{2ph} = [x\Delta p_v + (1 - x)\Delta p_\ell][1.5 - 0.5 \cos (2\pi x)]$$

This simple treatment of a complex problem can be justified to some extent. It does give a continuous variation of h_{2ph} and Δp for any quality x while some published relations are discontinuous. Its simplicity also permitted the development of the overall simulation to proceed. However, the prime justification for this approach is the

fact that accurate coefficients are not required in this case. Pressure drop is only a second order variable in a forced flow boiler so its accurate determination is not required. Also, the boiler under consideration is not heated by a constant heat flux source such as a nuclear reactor or electrical resistance. Instead, its heat is received from a combustion process through an outside coefficient that offers about 20 times the resistance to heat transfer that is offered on the water side. Thus the gas side coefficient dominates the heat flow and the steam side does not need to be determined accurately. Despite the arguments above, improvements in this area are needed.

3.5. Gas-side Relations

Gas-side correlations are entirely based on Kays and London (36). The gas-side coefficient h_g is given by

$$h_g = C_h \, C_p \, G \, Re^{-0.4} \, Pr^{2/3}$$

where C_h is a coefficient depending on the transverse tube spacing ratio $X_t = \frac{s_t}{d_o}$ and longitudinal ratio $X_\ell = \frac{s_\ell}{d_o}$ and is computed from

$$C_h = 0.0574 \, (X_\ell + 6.5) \, (X_t - 1)^{1/2}$$

The gas pressure drop for one coil is

$$\Delta p_g = f_g \frac{G_g^2}{2\rho}$$

where the friction factor is

$$f_g = 0.181\ (X_\ell + 1)\ (X_t - 0.86)\ Re^{-0.18}$$

The gas properties are given in Appendix B and the additional heat transfer due to radiation in the combustion chamber is covered in Appendix D.

As the gas flows from station m to station m+1 on the gas side of the tube wall, heat is transferred to the tube and the gas enthalpy drops. These variables are related by a gas-side steady-state energy equation:

$$\begin{matrix}\text{heat lost} \\ \text{to ambient}\end{matrix} + \text{heat transfer to tube} = \text{enthalpy drop of gas}$$

$$Q_L + Q_T = m_g\ \Delta\ h_g$$

or

$$C_L\ A_L\ (T_g - T_a) + h_g\ A_T\ \Delta\ T_{mean} = m_g\ (h_m - h_{m+1})$$

This equation is solved for $h_{g_{m+1}}$ which leads to $T_{g_{m+1}}$ (Appendix B).

3.6. Tube Temperature

In a transient simulation the variation in energy storage in the tube metal must be considered. The applicable relation is Fourier's Conduction Equation in cylindrical coordinates.

$$\frac{\partial T}{\partial t} = \alpha\ \frac{\partial^2 T}{\partial r^2} + \frac{\alpha}{r}\ \frac{\partial T}{\partial r} \qquad (3.21)$$

The method of solving this equation is independent of the solution to the PDE so it is given here. We write a Taylor series expansion for the gas side at point 1 of Fig. 3.1. We solve this for $\frac{\partial^2 T}{\partial r^2}$ and substitute in equation (3.21) to get:

$$\frac{\partial T}{\partial \tau} = \frac{2\alpha}{(\Delta r)^2} \left[T_2 - T_1 + \left(1 + \frac{\Delta r}{2r_1}\right) \Delta r \frac{\partial T}{\partial r}\right] \tag{3.22}$$

At the gas boundary where y is the convection coefficient the heat flux is

$$q = k \frac{\partial T}{\partial r} = y_g (T_g - T_1) + q_r$$

where q_r is the radiation flux. Define $C_1 = 1 + \frac{\Delta r}{2r_1}$.

Solve this equation for $\frac{\partial T}{\partial r}$ and substitute in equation (3.22)

$$\frac{\partial T}{\partial t} = \frac{2\alpha}{(\Delta r)^2} \left[T_2 - T_1 + C_1 \frac{\Delta r}{k} \{y_g (T_g - T_1) + q_r\}\right]$$

or in finite difference form

$$T_1' - T_1 = \frac{2\alpha\Delta t}{(\Delta r)^2} \left[T_2' - \left(1 + C_1 \frac{y_g \Delta r}{k}\right) T_1' + C_1 \frac{\Delta r\, y_g}{k} T_g + \frac{C_1 \Delta r}{k} q_r\right] \tag{3.23}$$

At point 2 the conduction law becomes

$$T_2' - T_2 = \frac{\alpha\Delta t}{(\Delta r)^2} \left[\left(1 + \frac{\Delta r}{2r_2}\right) T_1' - 2T_2' + \left(1 - \frac{\Delta r}{2r_2}\right) T_3'\right] \tag{3.24}$$

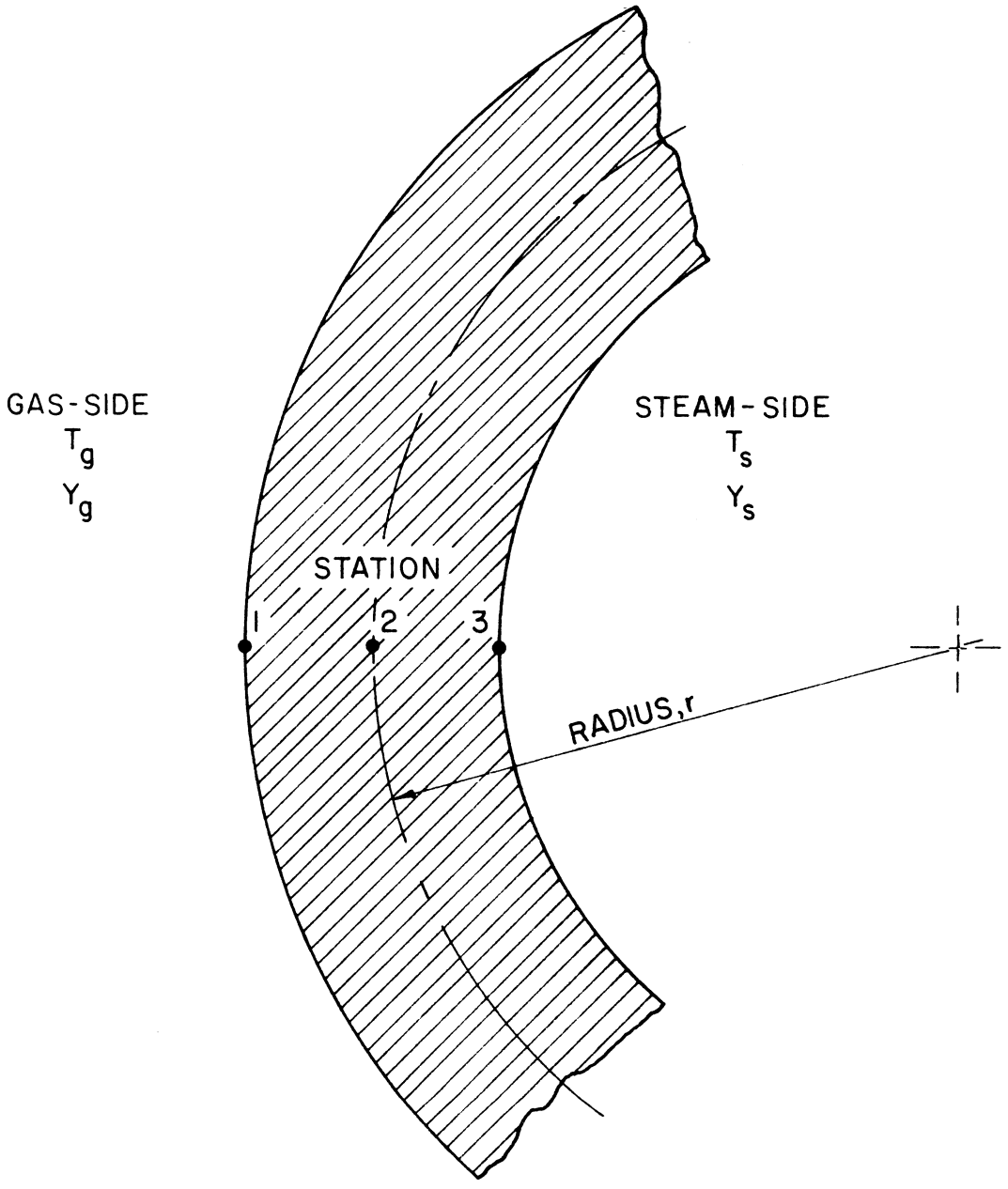

FIG. 3.1 NOMENCLATURE FOR ANALYSIS OF BOILER TUBE IN RADIAL DIRECTION.

Finally, on the steam side we employ the same method as used on the gas side with the Taylor Series expansion now at point 3 to get

$$T_3' - T_3 = \frac{2\alpha\ \Delta t}{(\Delta r)^2} \left[T_2' - \left(C_4 \frac{y_g\ \Delta r}{k}\right) T_3' + C_4 \frac{y_g\ \Delta r}{k} T_s\right] \qquad (3.25)$$

Where $C_4 = 1 - \frac{\Delta r}{2r_3}$ and primes indicate the <u>new</u> values and unprimed the old or former value. The last three equations may be put in matrix form and solved by determinants for the three unknowns T_1', T_2', and T_3'. These are the new tube temperatures and are evaluated at the center of each coil segment. Thus a boiler with n segments has n sets of three tube temperatures but it has n+1 sets of steam and gas properties.

IV. METHOD OF SOLUTION

The general relations in the last chapter are a set of non-linear partial differential equations (PDE) with variable coefficients. This complexity makes an analytical solution highly unlikely and we turn immediately to some method of approximation. Analog solutions of PDE are possible by lumping the variables in the space direction but a large facility is needed, hence we explore the possibilities of a digital simulation.

With reference to Fig. 5.1 (page 41), early in this research it was decided to let each spiral coil be represented by a single step in the space direction and to divide the helical coil into steps of approximately the same length. Following this philosophy the boiler of interest has 240 feet of tubing divided into only 17 segments. This mode of sub-division is convenient since all discontinuities in tube size and gas temperature occur between coils and a small number of steps leads to a more rapid solution. It is also realized that large step size leads to larger truncation errors.

4.1. Digital Simulation Considerations

A digital solution of PDE usually involves putting the equations in finite difference form. The result is a large set of quasi-linear equations hence the numerical solution of PDE is dependent on the solving of a matrix equation. Even before the finite difference equations (FDE) are written, some methods of solution may be considered.

A matrix equation may be solved by simple Jacobi iteration (37) provided the absolute value of all the eigenvalues of the coefficient matrix is less than 1.0. In essence, this requires diagonal dominance. This iterative method was discarded since the coefficients may vary by three orders of magnitude and thus convergence would be difficult to assure. It should be added here that the convergence of several other methods to be considered may be calculated based on eigenvalues but none of these methods have been employed since it is as easy to program the method itself and test it as it is to compute the eigenvalues for all possible conditions. Another method is to individually solve each set of equations. The FDE for each of the general equations form a matrix equation with a tri-diagonal coefficient matrix. For this particular situation the equations may be quickly solved using the Thomas alogrithm (38). This method has been successfully applied to 3-D boundary layers (39) and would probably serve for the present work. However, the separate solution of each conservation law means that the interaction between the laws is entirely dependent on iteration. In a boiler under some transient conditions this interaction is strong, hence we wish to calculate it as directly as possible. From this we conclude that the most direct method involves solving all three sets of equations simultaneously.

4.2. Steady Boiler Performance (SBP)

The first use made of the mathematical model was to neglect the time derivatives and solve the remaining ODE in order to evaluate

steady state performance. The SBP program has proven extremely useful since it is fast enough to permit parametric studies of boiler design and operating conditions and provides initial conditions for starting the Transient Boiler Performance (TBP) program.

Furthermore, it may be used to test TBP since the latter will eventually reach a steady operating state if all boundary conditions remain unperturbed. Though both simulations start from the same mathematical model, the method of solution is entirely different. To determine the steady performance of a given boiler SBP requires the economizer temperature, TSECON, the superheater outlet temperature, TBO, and the outlet pressure PBO. Then for a given steam rate, WDS, the program iterates on the gas flow rate, WDG, until the exit temperature is within a fraction of a degree of the specified value. Thus a "shooting" method is used to solve this two-point boundary value problem. The solution time is about 10 sec. per case compared with 20 min. for TBP.

4.3. Transient Superheater

In order to expedite programming and reduce computer time, the preliminary testing of methods of solution was done on a simplified model in which the ideal gas assumption was made on both sides of the tube wall and the pressure drop and heat transfer coefficients were constant.

The first method actually programmed was the Lax-Wendroff technique for solving the PDE in conservation form (38).

This is an explicit approach, i.e., the state at the next time point is expressed as an explicit function of the (known) state at the last time point so the FDE do not need to be solved simultaneously. This means the computation is simpler but the accompanying penalty is excessive computer time. This slow solution is caused by the small time step Δt which must be used to avoid computational instability. This penalty is severe--the time increasing by a factor of 10 or more for the cases examined. For this reason explicit methods of all kinds were dropped.

The second class of FDE are called implicit since the state at the next time point is dependent upon the forward (unknown) state of neighboring points as well as the previous state. Thus the equations are interdependent and must be solved simultaneously. Gary (40) offers some schemes which he calls implicit but stability conditions involving eigenvalues are imposed which is undesirable as has been explained. The first of Gary's methods is unconditionally stable but requires constant mesh size Δx which violates the ground rule given at the beginning of this chapter. He does make an interesting observation relative to the solution of the first order hydrodynamic flow equations for a polytropic gas. It appears that for this case with its variable coefficients, "... the specification of all dependent variables at <u>both</u> boundary points seemed to cause no trouble in our computations." Thus it appears that in some instances the boundary conditions can be over-specified with impunity. Gourlay and Morris (41) suggest improvements to Gary's method but a block tri-diagonal matrix must be inverted

and the step size question remains. The above methods were put aside in favor of the directly applicable approach presented by von Rosenberg (42). He combines the three sets of PDE into one large set having a tri-tridiagonal matrix. This matrix has a diagonal band 9 entries wide which can be solved using an algorithm introduced by Douglas. This technique was programmed, worked well on the transient superheater, and has been the mainstay of the steam work.

4.4. Steam Simulation (TBP)--New Problems

At this point in the proceedings it appears advisable to take a closer look at the PDE (equation (3.7) to equation (3.9)) which we are trying to solve. The first problem is that we have three differential equations and the four unknowns (v, u, p. h). One approach to this problem is to solve the PDE for 3 unknowns and then numerically calculate the derivatives involving the 4th unknown from the state equation data (steam tables). This notoriously noisy process was attempted for the $\frac{\partial p}{\partial x}$ term but the solution was not stable. A more promising scheme is to use the equation of state to remove one of the dependent variables from the PDE.

We note that the velocity, u, is a transport or momentum variable, not a thermodynamic variable, hence it cannot be expressed in a state equation as a function of the others. Thus we conclude that u must be one of the variables retained. Since the energy equation is dominant in this application it seems prudent to calculate its prime variable h directly rather than through linear approximations. The independent

variables in the steam tables are p and/or T so to retain one of them makes the steam table work easier, i.e., we have a simpler implicit relation to solve by iteration. However, T would not be satisfactory since $h \simeq c_p T$ in the superheat region thus h and T would not be independent there.

These arguments point to the retention of (u, p, h) as the dependent variables in the general laws. This means that v must be eliminated from the mass equation. We may write

$$v = f\ (p,\ h)$$

so

$$\frac{\partial v}{\partial t} = \left.\frac{\partial v}{\partial p}\right|_h \frac{\partial p}{\partial t} + \left.\frac{\partial v}{\partial h}\right|_p \frac{\partial h}{\partial t}$$

and

$$\frac{\partial v}{\partial x} = \left.\frac{\partial v}{\partial p}\right|_h \frac{\partial p}{\partial x} + \left.\frac{\partial v}{\partial h}\right|_p \frac{\partial h}{\partial x}$$

substituting these in the mass equation, equation (3.7) gives

$$\left.\frac{\partial v}{\partial p}\right|_h \frac{\partial p}{\partial t} + u \frac{\partial p}{\partial x} + \left.\frac{\partial v}{\partial h}\right|_p \frac{\partial h}{\partial t} + u \frac{\partial h}{\partial x} - v \frac{\partial u}{\partial x} = 0, \qquad (4.1)$$

The determination of the derivatives $\left.\frac{\partial v}{\partial p}\right|_h$ and $\left.\frac{\partial v}{\partial h}\right|_p$ is elementary for the magic world of the ideal gas where $pv = RT$ and $h = c_p T$. But for steam the problem is more involved as can be seen from the work in Appendix C.

4.5. Boundary Conditions

In an automotive boiler we are likely to know and/or control the water temperature and flow rate entering the boiler and the pressure leaving it. Thus for a boiler with n coils the boundary conditions (BC) are u_1, h_1 and p_{n+1} since the steam stations along the tube are numbered from the entrance. Now to use von Rosenberg's scheme, at a given station the subscript for a variable whose BC is at the exit must be one more than the subscript for a variable whose BC is at the entrance. Thus the subscripts for u and h range from 1 to n+1 while those for p range from 2 to n+2 as shown in Fig. 4.1. The BC for the gas temperature is T_{g_1} which is the combustion chamber temperature (Appendix B).

4.6. Finite Difference Equations (FDE)

We note that all derivatives will be approximated by four numbers representing the station number at each end of the coil and the next (primed) and last (unprimed) point in time as depicted on the time-space plot in Fig. 4.2. The mean of these four numbers is, e.g., $\bar{p}$.

The FDE corresponding to equation (4.1), (3.8) and (3.9) are:

$$\left.\frac{\partial \bar{v}}{\partial p}\right|_h \left[\frac{p'_i + p'_{i+1} - p_i - p_{i+1}}{2\Delta t} + \bar{u}\ \frac{p'_{i+1} + p_{i+1} - p'_i - p_i}{2\Delta x}\right] +$$

$$\left.\frac{\partial \bar{v}}{\partial h}\right|_p \left[\frac{h'_{i-1} + h'_i - h_{i-1} - h_i}{2\Delta t} + \bar{u}\ \frac{h'_i + h_i - h'_{i-1} - h_{i-1}}{2\Delta t}\right] -$$

$$\bar{v}\left[\frac{u'_i + u_i - u'_{i-1} - u_{i-1}}{2\Delta x}\right] = 0$$

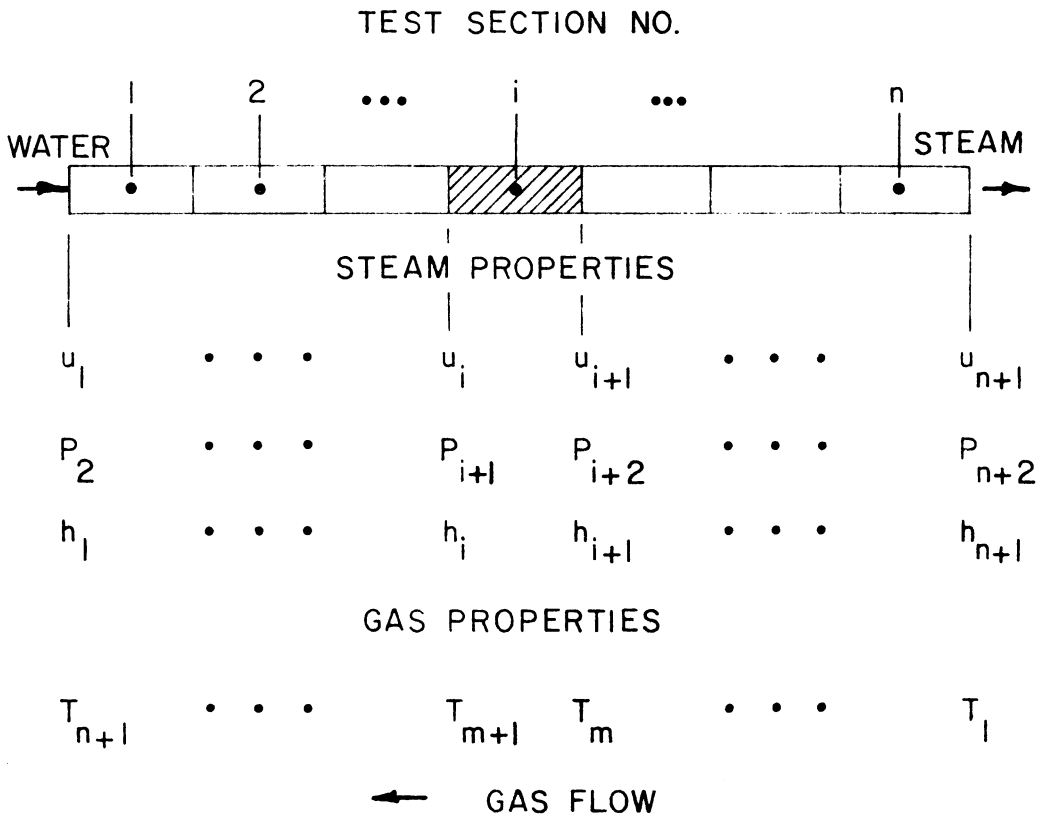

FIG. 4.1 NOMENCLATURE FOR ANALYSIS OF BOILER TUBE IN LONGITUDINAL DIRECTION.

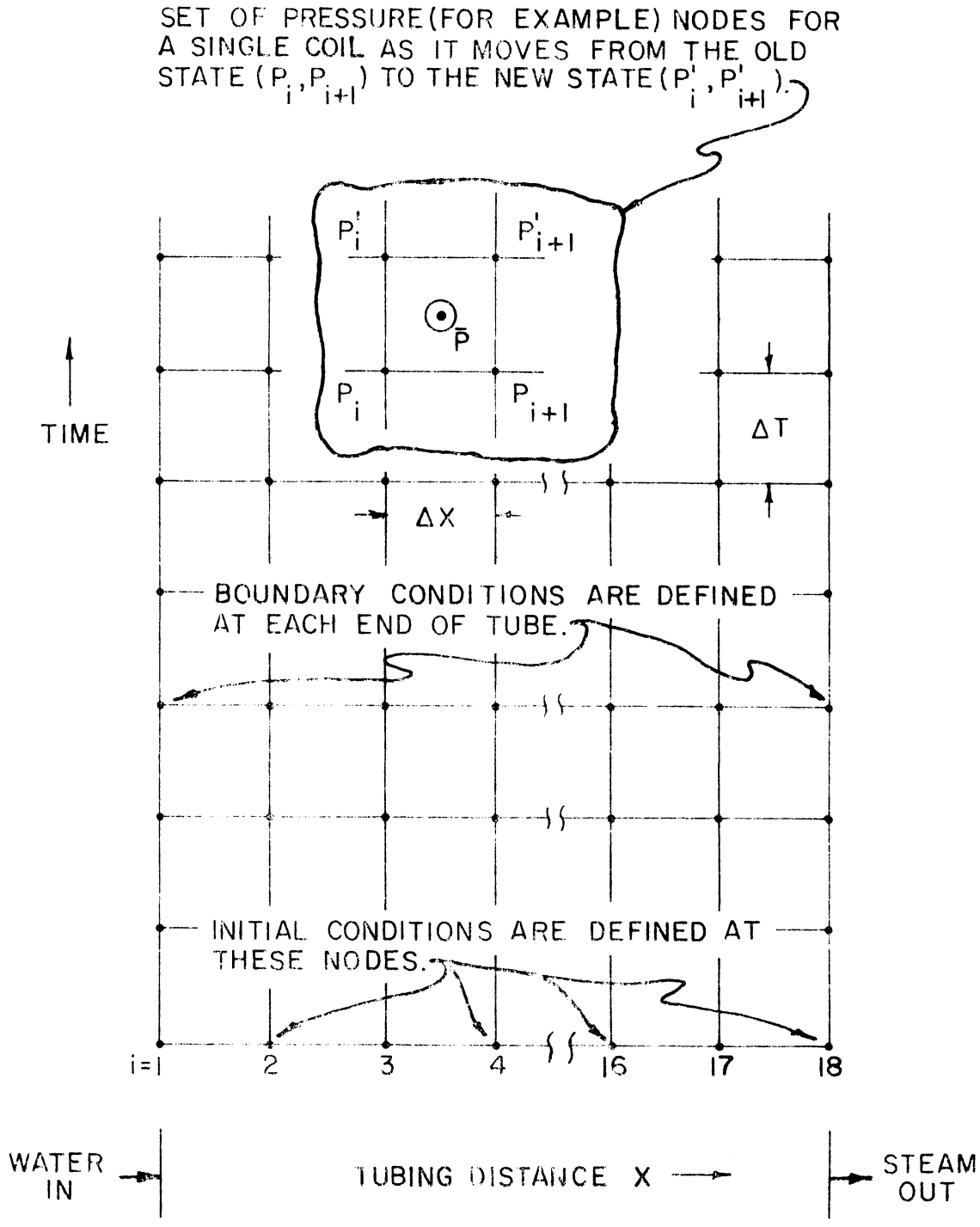

FIG. 4.2 FINITE DIFFERENCE DEFINITIONS

and

$$\frac{u'_{i-1} + u'_i - u_{i-1} - u_i}{2\Delta t} + \bar{u}\ \frac{u'_i + u_i - u'_{i-1} - u_{i-1}}{2\Delta x}$$

$$+ \bar{v}\ \frac{p'_{i+1} + p_{i+1} - p'_i - p_i}{2\Delta x} = \bar{v}\ \frac{\partial p_f}{\partial x}$$

and

$$\frac{h'_{i-1} + h'_i - h_{i-1} - h_i}{2\Delta t} + \bar{u}\ \frac{h'_i + h_i - h'_{i-1} - h_{i-1}}{2\Delta x} + \bar{u}\ [\frac{u'_{i-1} + u'_i}{2\Delta t}$$

$$\frac{- u_{i-1} - u_i}{}] + \bar{u}^2\ \frac{u'_i + u_i - u'_{i-1} - u_{i-1}}{2\Delta x} - \bar{v}\ \frac{p'_i + p'_{i+1} - p_i}{2\Delta t} -$$

$$\frac{p_{i+1}}{} = \bar{v}\ (\frac{Q}{V} - \bar{u}\ \frac{\partial p_f}{\partial x})$$

We multiply through by $2\Delta t$, define $a = \frac{\Delta t}{\Delta x}$, $b = 1 + a\bar{u}$, $c = 1 - a\bar{u}$, collect terms and put all the new variables on the left hand side (LHS)

$$a\bar{v}u'_{i-1} - a\bar{v}u'_i + \left.\frac{\partial \bar{v}}{\partial p}\right|_h cp'_i + \left.\frac{\partial \bar{v}}{\partial p}\right|_h b\ p'_{i+1} + \left.\frac{\partial \bar{v}}{\partial h}\right|_p ch'_{i-1} + \left.\frac{\partial \bar{v}}{\partial h}\right|_p bh'_i$$

$$= a\bar{v}\ (u_i - u_{i-1}) + \left.\frac{\partial \bar{v}}{\partial p}\right|_h (b\ p_i + c\ p_{i+1}) - \left.\frac{\partial \bar{v}}{\partial h}\right|_p (b\ h_{i-1} + ch_i), \tag{4.2}$$

and

$$cu'_{i-1} + bu'_i - a\bar{v}\ p'_i + a\bar{v}\ p'_{i+1} = bu_{i-1} + cu_i + a\bar{v}\ (p_i - p_{i+1})$$

$$+ 2\Delta t\bar{v}\ \frac{\partial p_f}{\partial x} \tag{4.3}$$

and

$$\bar{c}\bar{u}\, u'_{i-1} + b\bar{u}\, u'_i - \bar{v}\, p'_i - \bar{v}\, p'_{i+1} + ch'_{i-1} + bh'_i =$$

$$\bar{u}\,(bu_{i-1} + cu_i) - \bar{v}\,(p_i + p_{i+1}) + bh_{i-1} + ch_i + 2\Delta t\bar{v}$$

$$(\frac{Q}{V} - \bar{u}\,\frac{\partial p_f}{\partial x}) \qquad (4.4)$$

Equations (4.2) through (4.4) are now written for each coil to give a set of 3(n+1) simultaneous equations which are readily solved using the Douglas algorithm given by von Rosenberg.

Since the general equations have variable coefficients, the program iterates once to update them and increase accuracy. It was found that 2 or 3 iterations did not alter the results appreciably.

4.7. Simplified Solutions

In an effort to reduce computer time some less complex models have been examined. A 2-equation version (Program No. 2) solves the momentum and energy equations simultaneously for p and h but the derivatives in u and v are evaluated numerically. This numerical differentiation of computer data is such a noisy process that arbitrary limits had to be placed on the derivatives to obtain a solution. These limits restrict the simulation's ability to follow a rapid transient.

A one-equation version (Program No. 1) solves only the energy equation in transient form. The time derivatives in the other equations are neglected entirely, hence there is no numerical differentiation.

Results from these three programs are compared in Chapter VI where it is shown that large differences are obtained, hence only the more complete and accurate 3-equation version (Program No. 3) is discussed in detail.

V. EXPERIMENTAL APPARATUS

Some preliminary experimental data to validate the computer simulation were obtained with the apparatus briefly described below.

5.1. Boiler

The boiler consists of an oil-fired combustion chamber within a closely wound helical coil of 0.5-in. dia type 321 stainless steel tubing, (Fig. 5.1). Hot gases leaving the chamber pass through 10 loosely wound spiral coils of tubing to the exit flue. Feed water enters the coil nearest the flue and passes from coil to coil until it emerges from the combustion chamber end as superheated steam. Thus the steam passes only once through a single tube 240-ft long. The completed boiler was hydraulically tested to 2400-psi which was the limit of the available pump.

These coils are enclosed in a casing of 0.037-in. 321 stainless sheet and 1.0-in. of insulation (Behr-Manning 1800 F mineral board).

5.2. Burner

The burner mixes fuel and air in a central flame tube within the spiral coils and blows this burning mass into a stainless can which serves as a liner in the combustion chamber. This liner protects the tubes from direct flame impingement and turns the gases 180° to flow back through the spiral coils to the flue. A 1.0-hp, 1.0-psi blower was used to force air through a 1-3/4-in. S.U. carburetor with a

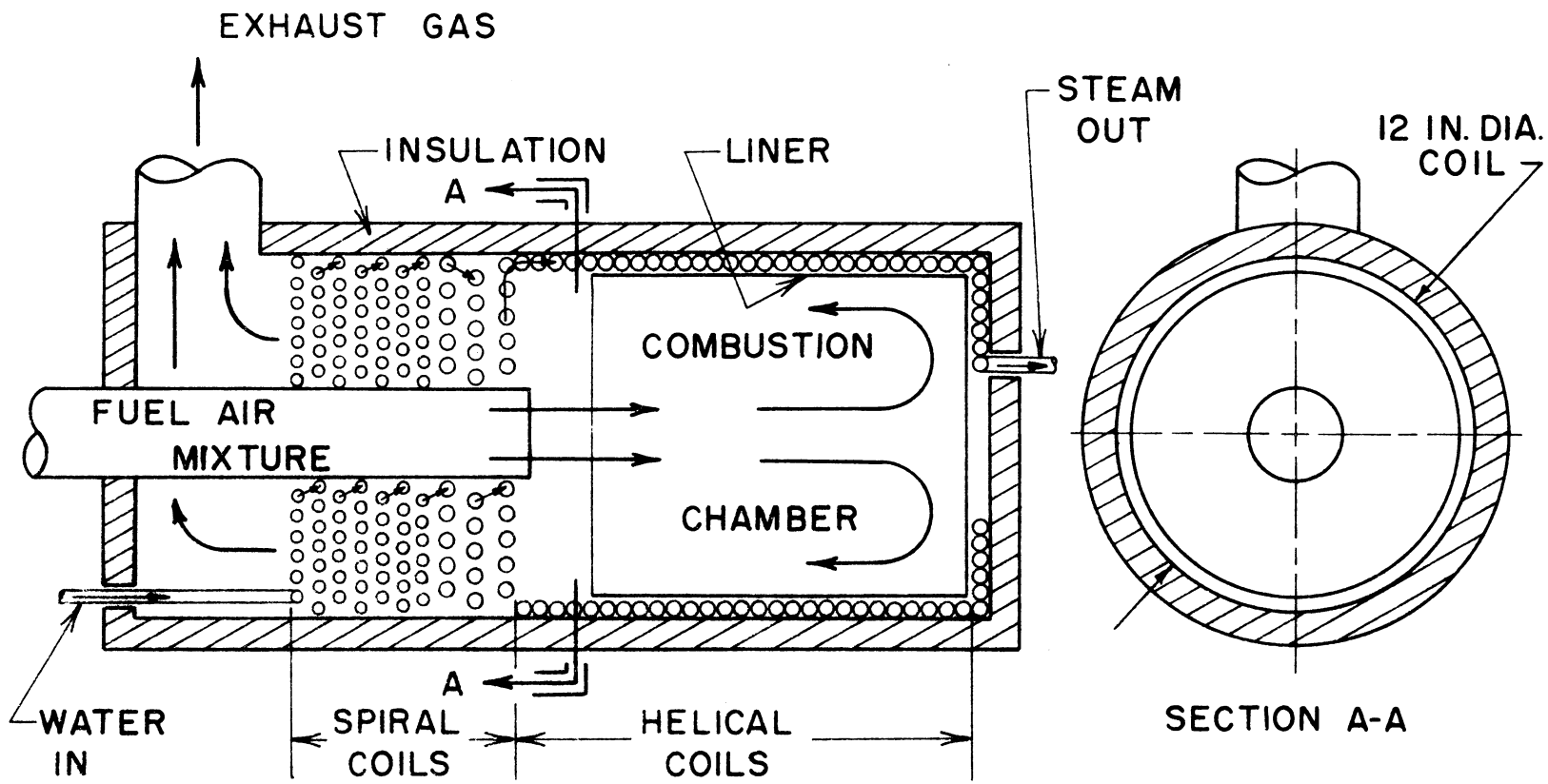

FIG. 5.1 EXPERIMENTAL BOILER LAYOUT

balanced float bowl but this carburetor burner was abandoned since the maximum steam rate was only 100 lbm/hr.

The second burner was an experimental air-atomizing type with an offset (tangential) entrance which gave the air in the 3-in. dia flame tube a swirling motion. A spoiler in the inlet permitted control of the swirl rate. A cross shaft upstream of the spoiler carried a butterfly valve to control air flow rate and a cam to operate a needle valve which controlled fuel flow rate. Vernier control of the needle valve permitted small corrections to be made to the A/F ratio.

The boiler feed pump was a 1000-psi, 5-gpm triplex made by Cat Pumps and was driven through a variable ratio V-belt drive by a 2-hp motor.

5.3. Instruments

Boiler inlet and outlet pressures were measured with a 1500-psi bourdon tube gage with switching valves. Water inlet, steam outlet and flue gas temperatures were determined with thermocouples and a direct reading galvanometer with an automatic compensator for varying ambient temperatures. An ASME orifice with a water manometer gave the air flow rate and a stop watch in conjunction with a 300-cc bulb gave the flow rate of #2 fuel oil. The gas pressure drop across the spiral coils was measured with a water manometer. Water flow rate was measured with a tapered tube flow meter.

Figure 5.2 shows the layout of the apparatus. The boiler is the large 14-in. dia x 26-in. long cylinder on the lower shelf of the

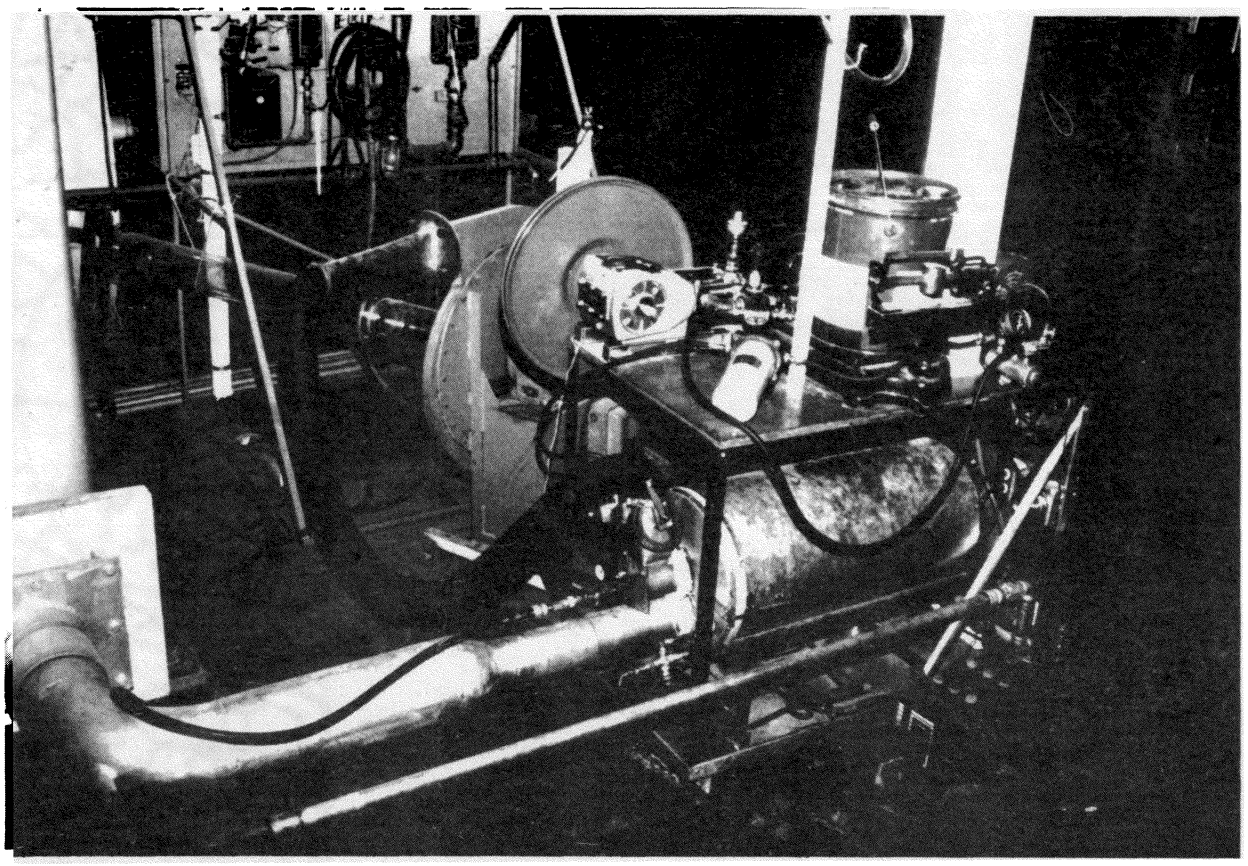

Fig. 5.2 Experimental apparatus - stack side

24 x 42-in. cart. It discharges flue gas and steam horizontally to the 24-in. dia stack on the left edge of the figure. The boiler feed pump with its large 19-in. dia V-pulley is mounted on the left-most corner of the upper shelf of the cart. This pulley partly obscures the blower, though the 3-in. dia flexible air hose leading to the burner is easily seen. The fuel supply system is also mounted on the upper shelf. It consists of a 5-gal fuel can on a scale, a glass measuring bulb mounted in the large, white vertical column in the upper right, a Bendix electric fuel pump on the right-most corner, and a fuel filter on the nearest corner. The control panel in the upper left is not part of this apparatus.

Figure 5.3 is a view of the apparatus from the opposite side. On the right side is seen the blower, the air flow orifice and inlet tube passing out of the picture at right center and the stack behind the blower. On the upper shelf of the cart on the left side of the photograph is seen the pump, its motor, and the variable speed drive between them. On the instrument panel in the lower left a rectangular temperature gage, 6-in. dia pressure gage and the tapered tube flow meters can be seen. Switches, steam throttle, and water bypass valve are also located on this panel.

With the exception of the low combustion efficiency discussed in Chapter VI this experimental rig operated without failure or other difficulty for about 30 hours.

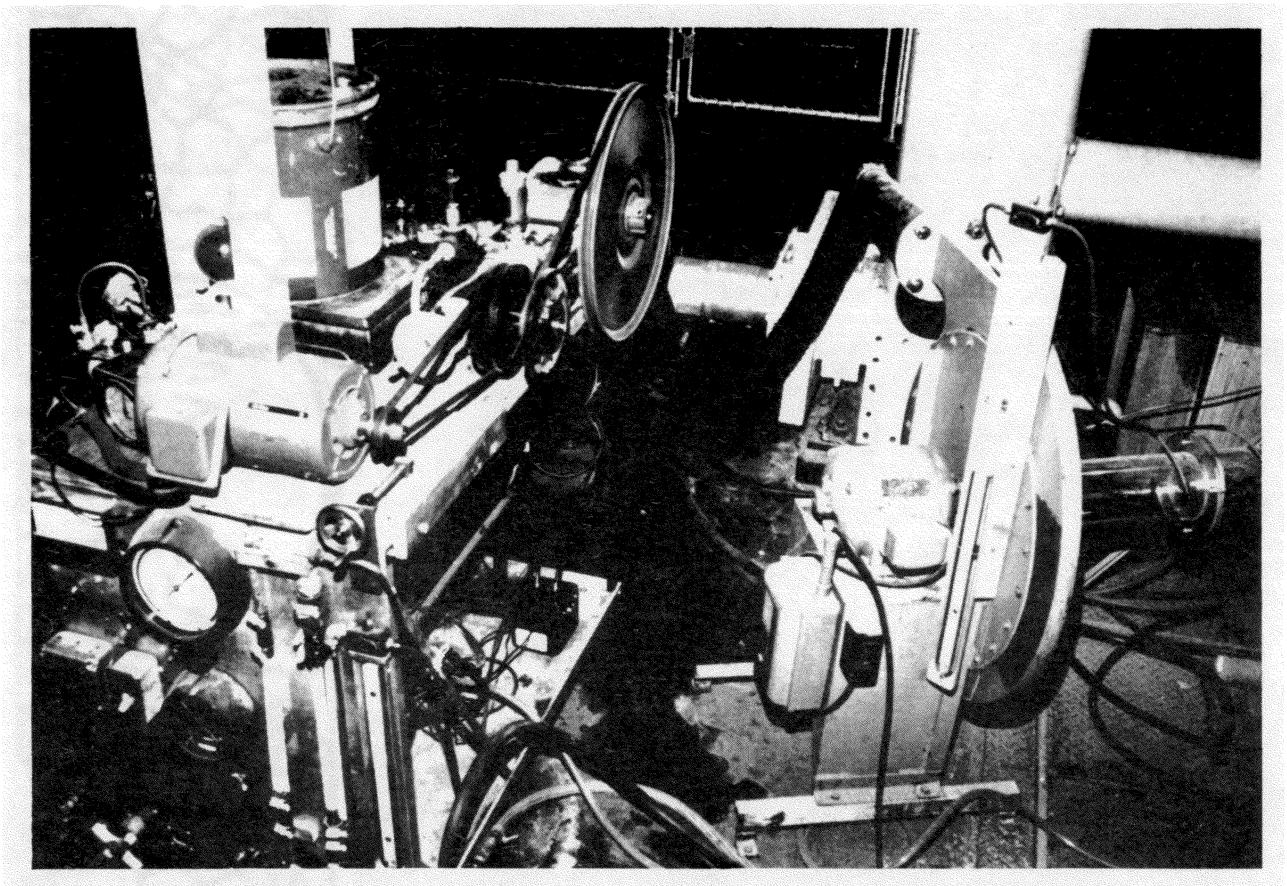

Fig. 5.3 Experimental Apparatus - instrument side

VI. RESULTS AND DISCUSSION

The mathematical model of a monotube boiler given in Chapter III has been programmed in Fortran using the method of solution developed in Chapter IV. Some of the attendant birth pangs are described in the present chapter before giving some of the results from the final program.

6.1. Simulation Development

Implicit FDE solutions are usually considered to be stable but time step size is limited by truncation errors. Throughout this research effort the largest allowable time increment, Δt, has been employed. While this increases the truncation, i.e., the error resulting from approximating a curve with a straight line, a large Δt reduces the computer time. This advantage not only reduces the cost of research but permitted the program to be run on occasions when a longer job time would have caused the job to be shunted aside into a standby status.

In order to further reduce computation time a variable step size has been adopted. Unlike the predictor-corrector techniques used to solve ODE, the FDE employed here are based on the state of the system at the last time point but not on the state previous to the last point. This means that no special methods are required to "start" the solution hence there is no penalty attached to varying the increment at every step if desired. From the several methods that were considered for estimating the new step size, $\Delta t'$ the following was chosen:

$$\Delta t' = \frac{\Delta t}{0.90 + C \times R} + \Delta t_{min}$$

where Δt is the previous step size and R is the average relative change of specific volume and enthalpy during the last step and is given by

$$R = \left\{ \sum_{i=1}^{n+1} \left| \frac{v_i'}{v_i} - 1 \right| + \sum_{i=1}^{n+1} \left| \frac{h_i'}{h_i} - 1 \right| \right\} \frac{1}{2(n+1)}$$

and the constant C governs the step size used and is usually chosen to be about 500 in order to eliminate spurious fluctuations in outlet temperature due to excessive truncation error. The minimum time, Δt_{min}, prevents Δt from falling below some minimum value, usually 0.001 sec.

It can be seen that if there is a large change of state during the last step then R will be large and Δt will be reduced relative to the last value.

The most vexing problem of this research was caused by the partial derivatives used to introduce the equation of state directly into the governing equations (Sec. 4.4). The difficulty arises because these derivatives are discontinuous at the saturation lines. The worst offender is $\left.\frac{\partial v}{\partial h}\right|_p$ which can change by a factor of 1000 at the saturated liquid line. A step function of this magnitude simply cannot be successfully accommodated by a digital computer so a means was sought to ease the transition over the saturation lines. The method adopted rests on the key observation that the enthalpy increases with distance along the boiler tube in a smooth, gradual manner even at saturation. If we assume a linear variation in enthalpy in a tube section then the length fraction, F, at which evaporation starts is

$$F = \frac{h_{out} - h_{sat}}{h_{out} - h_{in}}$$

This fraction is then used to calculate the weighted average derivative in the same manner that steam quality is used to calculate other thermodynamic properties within the two phase region. The relation used is

$$\left.\frac{\partial v}{\partial h}\right|_p = F \left.\frac{\partial v}{\partial h}\right|_{p_{out}} + (1 - F) \left.\frac{\partial v}{\partial h}\right|_{p_{in}}$$

An analogous expression is used for $\left.\frac{\partial v}{\partial p}\right|_h$. Far more sophisticated techniques for crossing saturation have been tested without any success.

6.2. Comparison of Steady and Transient Programs

As a first step in checking out TBP it was run for 120 sec without changing any boundary condition. For the boiler modeled herein this represented approximately an equilibrium state. This steady state was then compared with that predicted by SBP. For the test case of 300 lbm/hr of 400 psia steam from 130 F feedwater, the exit enthalpies differed by 26 B/lbm even though the Air/Fuel flow rates were the same. This large difference was caused by the omission of the viscous dissipation term in the energy equation in the SBP program. This experience inadvertently pointed out that the viscous term cannot be ignored in an accurate simulation. When it was added, the programs differed by less than 4 B/lbm in exit enthalpy and 4 psi in inlet

pressure which is judged a reasonable discrepancy in view of the variation between the methods of solving the difference equations.

The simplified one- and two-equation versions of the transient model were also within the same bounds.

This close agreement of four programs using distinctly different methods of solution gave confidence that the mathematical model was being exercised correctly.

6.3. Response to Step Inputs

In order to build confidence in this simulation it is necessary that it compare favorably with experimental data. Unfortunately, no really detailed description of a monotube boiler and its test results has been found in the literature. Empirical data are available but the thorough description of the boiler that is needed for this simulation has not been included. For this reason only qualitative comparisons are offered in this section.

All the transient runs reported here started with the boiler delivering steam under steady conditions. The first set of runs compares the response of the 17-coil automotive boiler of interest to a 10% increase in input water flow rate. The resulting change in outlet enthalpy as predicted by the three transient programs is given in Fig. 6.1. We immediately note the large differences among the curves. Some differences in results are to be expected in view of the differences in the programs that produced them (Sec. 4.7) but this comparison gives the first evidence of the large magnitude of the

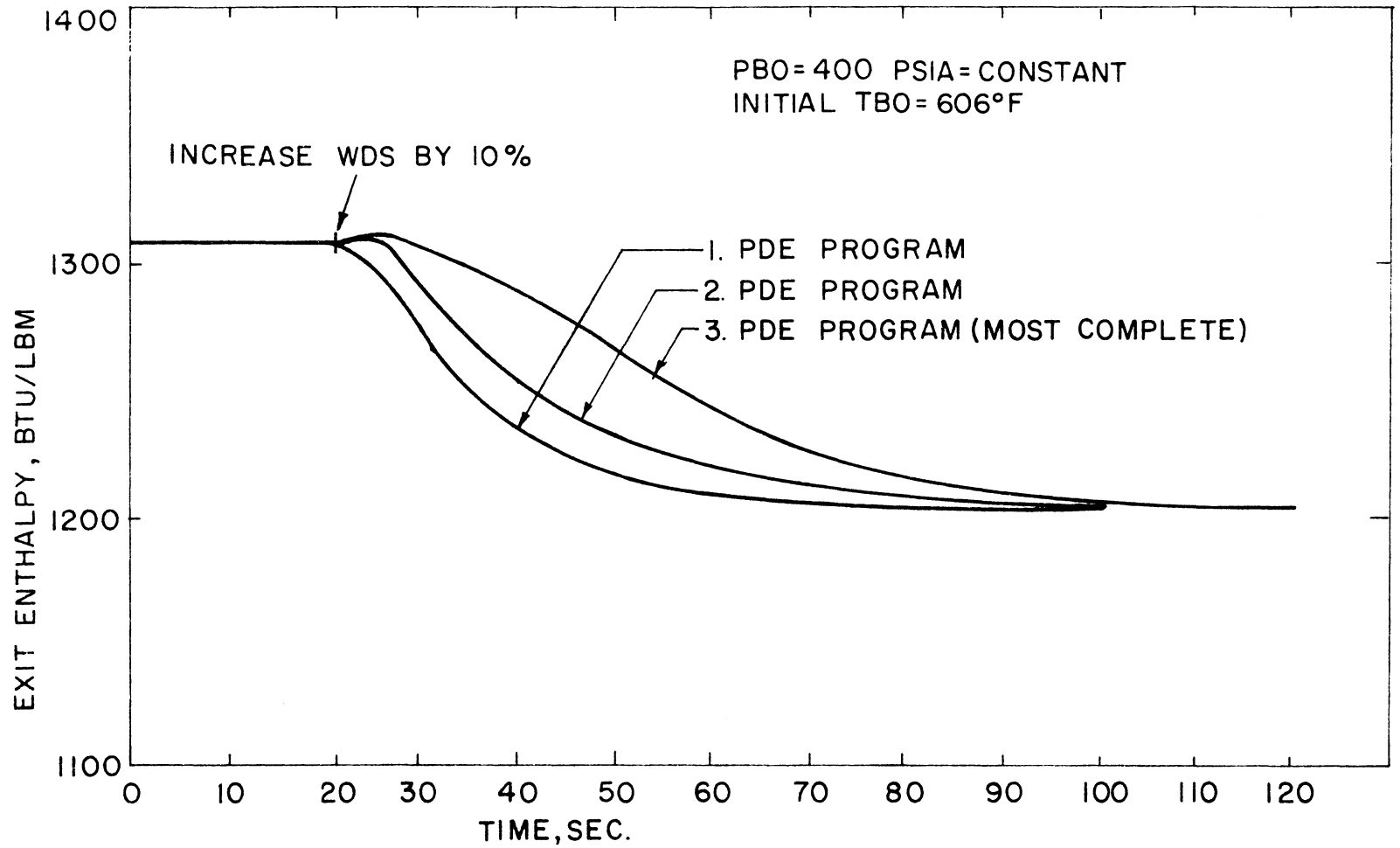

FIG. 6.1 THE EFFECT OF A 10% INCREASE IN WATER RATE AS PREDICTED BY THREE SIMULATIONS

variations. Program No. 3 is the most complete so it is expected to give the most accurate results. For this reason the simple programs have been de-emphasized and will not receive much attention in the remainder of this work.

As a result of a step increase in water rate, the exit enthalpy falls in a curve that could be crudely approximated by a pure delay of about 15-sec followed by an exponential decay as used by Peoples (25).

The effects of changes in water and fuel flow rates are compared in Fig. 6.2. It is seen that a 20% step decrease in fuel flow causes a slower fall in boiler outlet temperature TBO than a 20% increased water flow. This result is initially surprising in view of the fact that cutting the fire completely on the test rig caused the pressure to plummet from 800 to 600-psi in only 5.5-sec. The explanation of these diverse results lies in the difference in boundary conditions. The experimental boiler was discharging through a choked throttle valve of constant flow area while the simulation results in Fig. 6.2 (and Fig. 6.1) pertain to a constant discharge pressure, PBO.

If PBO is held constant a decrease in fuel flow causes a large decrease in flow rate, WDS. This temporary reduction in WDS is accompanied by a draining of the stored energy in the tube wall which maintains the high temperature steam flow for a longer period of time since there are fewer lbm of steam per sec to convect the energy away. The lower WDS also explains the 5 F temperature rise in the first few seconds after the step. When the water feed rate increases, the flow

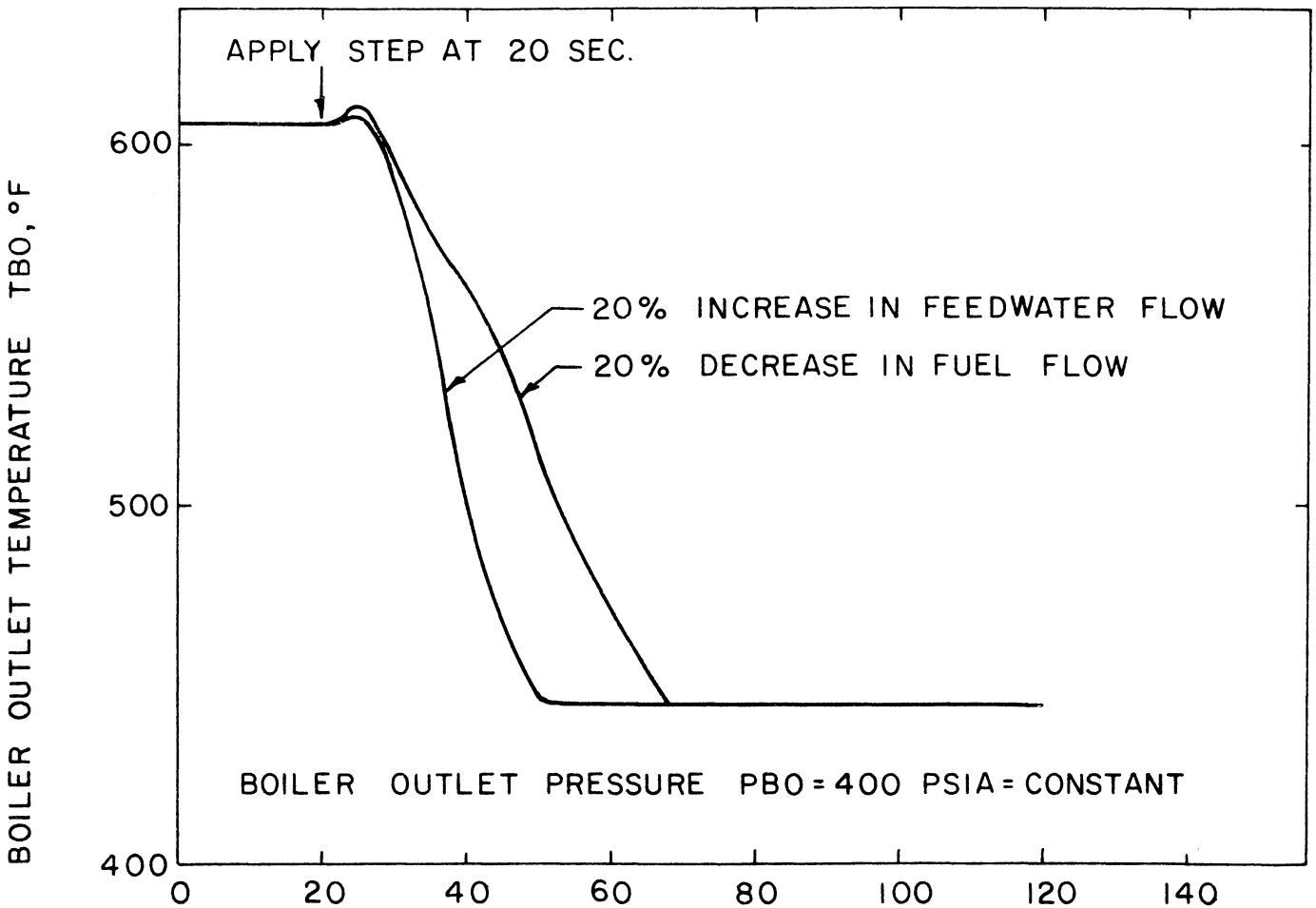

FIG. 6.2 EFFECT OF STEP CHANGES IN WATER AND FUEL FLOW

does not decrease at any point in the boiler. The higher flow increases the heat transfer from the tube wall. It also increases the friction pressure drop through the tube with the result that the pressure, and hence, temperature in the boiling region, increase. This increased heat transfer and saturation temperature combine to raise the steam temperature 2 F about 5-sec after the step increase in water flow. Thus the transients in Fig. 6.2 appear reasonable if one accounts for the constant pressure boundary condition.

As the next step in exercising the TBP simulation a choked flow outlet condition was imposed. This requires an equation relating the area of the throttle valve, A_v, to the thermodynamic variables p, v, and T which are found in the tube just upstream of the nozzle or valve. Since we are only interested in superheated steam the ideal gas assumption can be made and the mass flow m is

$$m = \frac{p\, A_v}{\sqrt{T}}\, f(\gamma,R)$$

where $f(\gamma,R)$ is primarily a function of the fluid and is considered constant. From continuity we may also write the mass flow in terms of tube area, A_t, and steam velocity in the tube u

$$m = \frac{u\, A_t}{v}$$

Equating these expressions gives

$$p = \frac{c}{v} \left(\frac{u}{A_v/A_t}\right)^2$$

This equation permits determination of the outlet pressure boundary condition for choked flow as a function of the outlet velocity, specific volume and the relative throttle valve area ratio A_v/A_t.

Figure 6.3 gives the variation in outlet temperature for a step change in feed water flow rate when a choked exit is used. (Note that Fig. 6.2 and Fig. 6.3 are not comparable since the boiler simulated had different initial and boundary conditions). We note that the temperature reaches a minimum at 120 sec and then slowly rises. This is caused by a transient flow rate which exceeds the inlet rate in most segments of the boiler from 80 sec on. This excessive flow reduces TBO in the 80-120 sec period but as this excess decreases and an equilibrium flow is approached TBO begins to rise toward its steady value (Fig. 6.4).

6.4. Response to a Sinusoidal Input

The frequency-response of a system is determined by subjecting it to sinusoidal input perturbations of varying frequency and observing the resulting output amplitude and phase change. As a check on the simulation's ability to handle these repetitive disturbances it was programmed for a sinusoidal variation in inlet water flow. Hess and co-workers (23) have found that if the amplitude of the perturbations is limited to 6% of the mean value a monotube boiler has a linear response. This means that an input signal is reproduced as an undistorted output. Thus we could expect a linear boiler to give a sinusoidal output if perturbed by a sinusoidal input. To be specific,

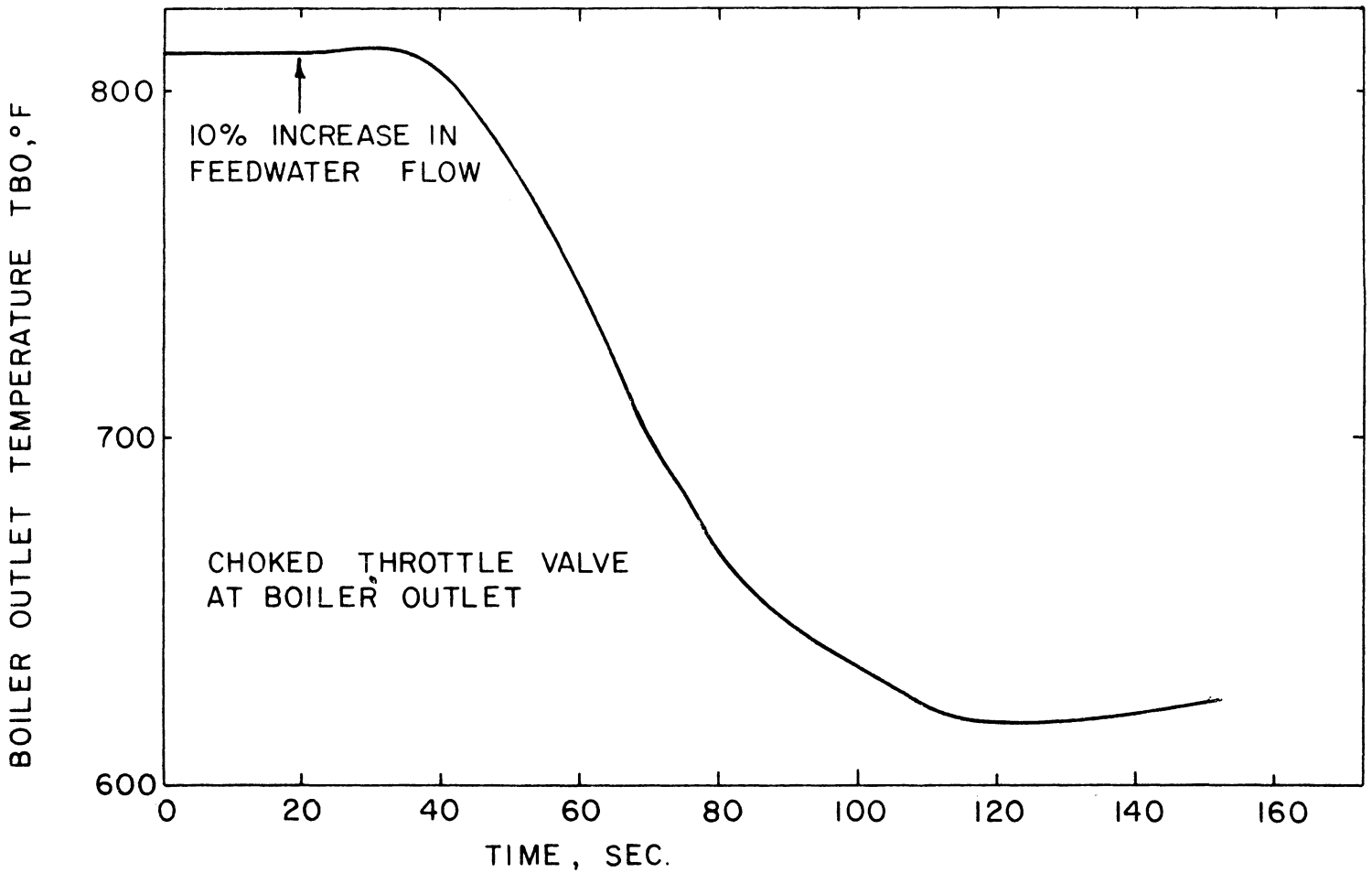

FIG. 6.3 EFFECT OF A STEP CHANGE IN WATER FLOW WITH A CHOKED OUTLET

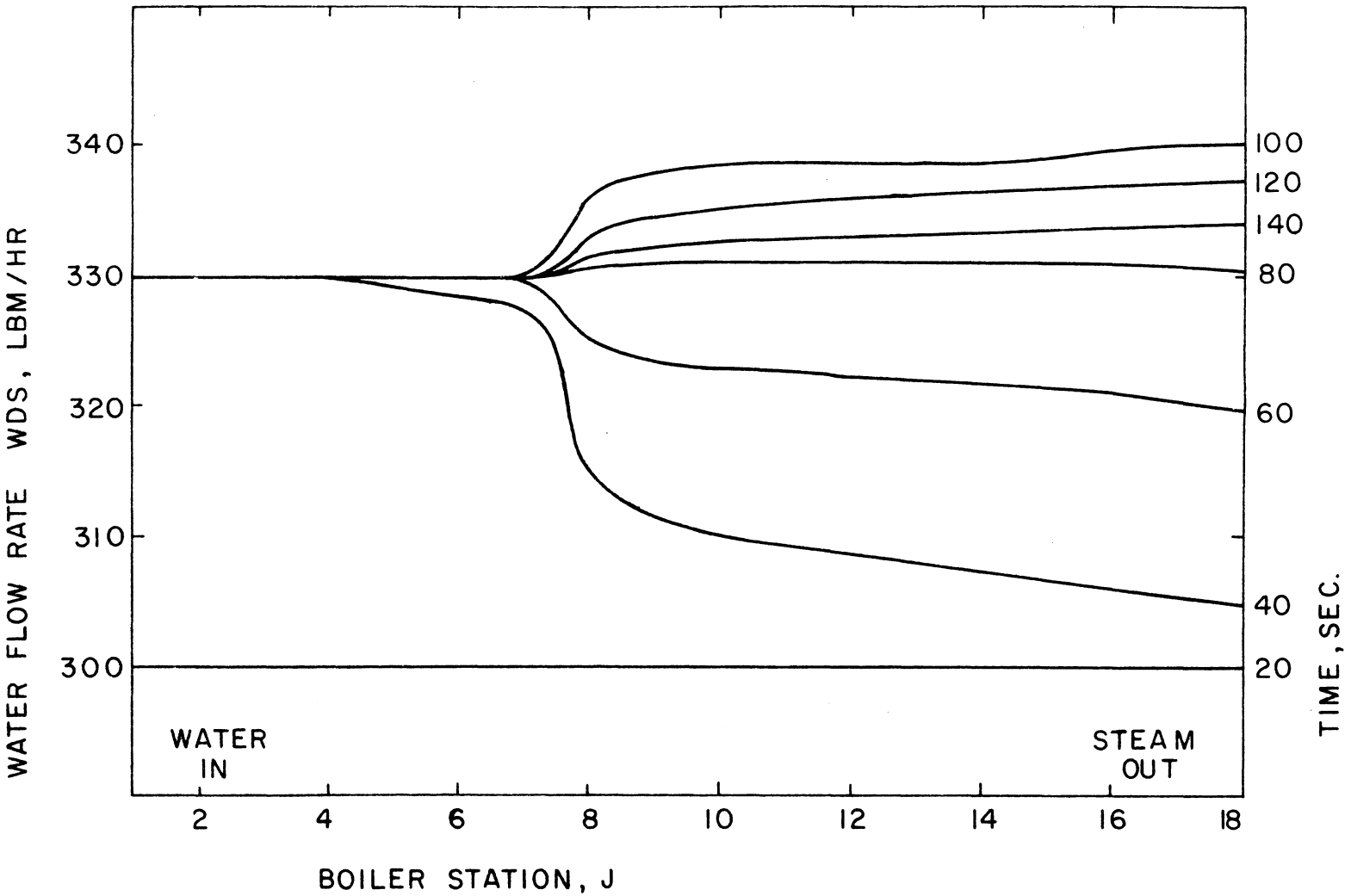

FIG. 6.4 WATER FLOW VARIATION ALONG LENGTH OF BOILER TUBE

Hess found that his test boiler gave a sinusoidal variation in boiler outlet temperature TBO in response to a sinusoidal variation of inlet water flow. This same situation was tested on TBP with the results given in Fig. 6.5. The boiler was operating under steady conditions until the perturbation was started at 20 sec. We observe that after about three cycles (180 sec) TBO has settled down to what appears to be a sine wave. Since TBO falls when WDS increases, a comparison of the TBO and WDS curves shows that the temperature is lagging the driving function by 39 sec or 234°. The amplitude of the TBO variation is about 10 F while a 6% change in water flow would cause a steady state change of 50 F. Thus the amplitude ratio is about 0.2 so operation is stable at this frequency and probably would be at the critical frequency which gives a phase lag of 180°. It is worth noting that Hess never found a resonant frequency at which the boiler was unstable, i.e., the amplitude ratio greater than 1.0.

From the data in Fig. 6.5 it is concluded that TBP is capable of simulating a boiler subjected to sinusoidal inputs.

6.5. Comparison with Steady Experimental Data

The aforementioned paucity of complete test data on small monotube boilers prompted the building of the unit described in the last chapter. This boiler has undergone preliminary testing and the results will be compared with those predicted by the simulation.

Boiler efficiency is a fundamental measure of steam generator performance. It is the ratio of the thermal energy actually received

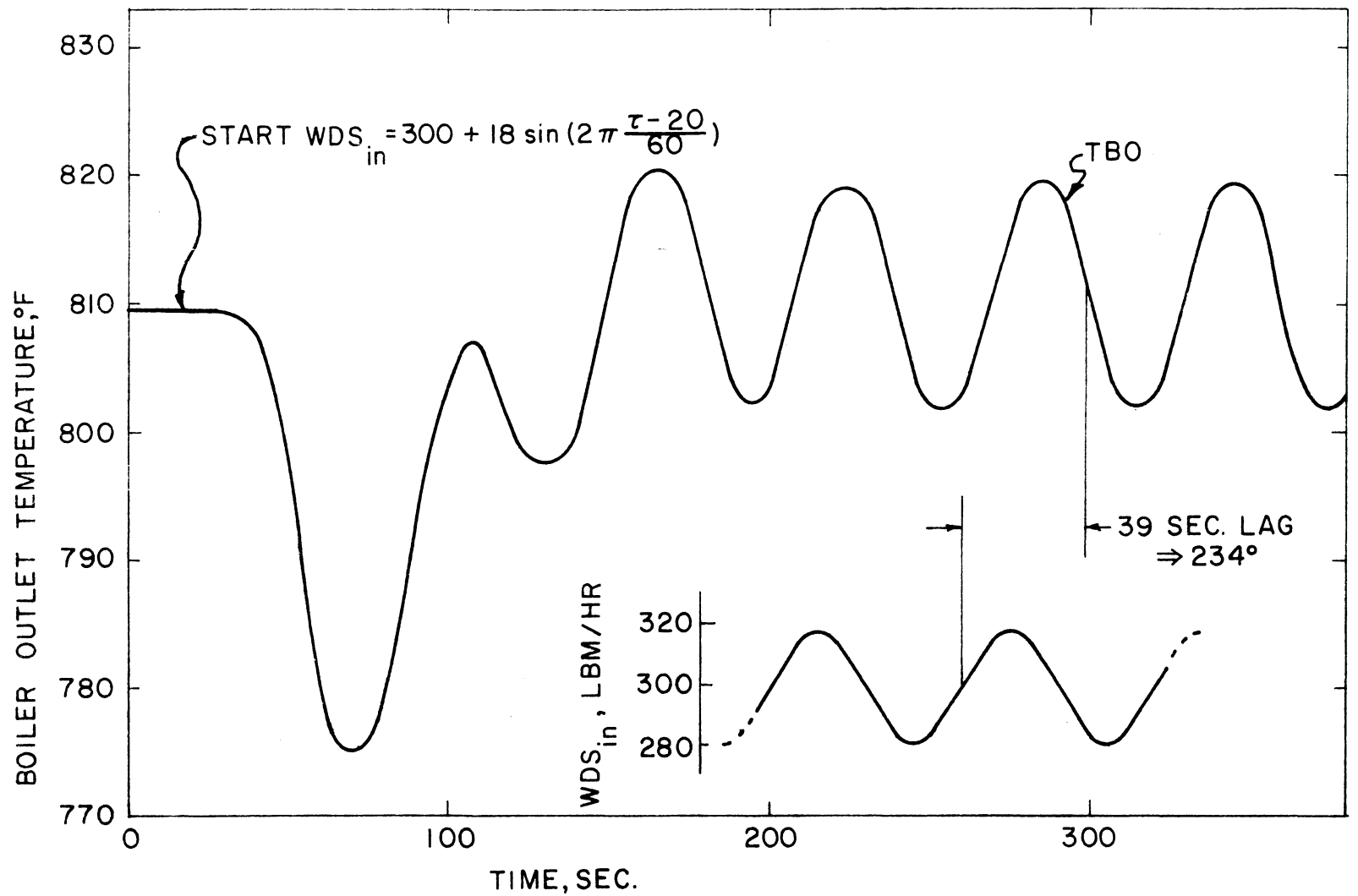

FIG. 6.5 BOILER OUTLET TEMPERATURE FOR A SINUSOIDAL VARIATION OF INLET WATER FLOW

by the steam to the chemical energy available in the fuel and may be computed from

$$\eta_b = \frac{m_s\ (hs_{in} - hs_{out})}{m_f\ HV_f}$$

This efficiency is plotted in Fig. 6.6 for the 13 data points available. The variation of η_b at a given steam rate is largely a result of varying steam conditions between points. However, the extremely peaked shape of the overall curve demands further investigation. A boiler efficiency of 75% at 250 lbm/hr was expected for this design (with its small number (10) of widely spaced coils) but the rapid deterioration in performance at steam rates on both sides of this maximum was disappointing. The difference between predicted and measured efficiency is given in Fig. 6.7. For steam rates in the 200-300 lbm/hr range, the difference is small (about 2%) for most points. At higher rates the difference of about 10% may be explained by incomplete combustion. When the nozzle and flame tube were tested outside the boiler, drops of liquid fuel were observed falling from the end of the tube at high fuel rates. In the boiler this fuel would fall to the bottom of the casing, evaporate, and be blown out with the flue gas without burning at all. The thesis of incomplete combustion is further substantiated by the sooty appearance of the coils when they were examined after the test. Since the program assumes 100% combustion efficiency it naturally predicts higher η_b than was measured.

The main problem is explaining the drop in η_b at low steam rates. This also could be explained by poor combustion but separate testing

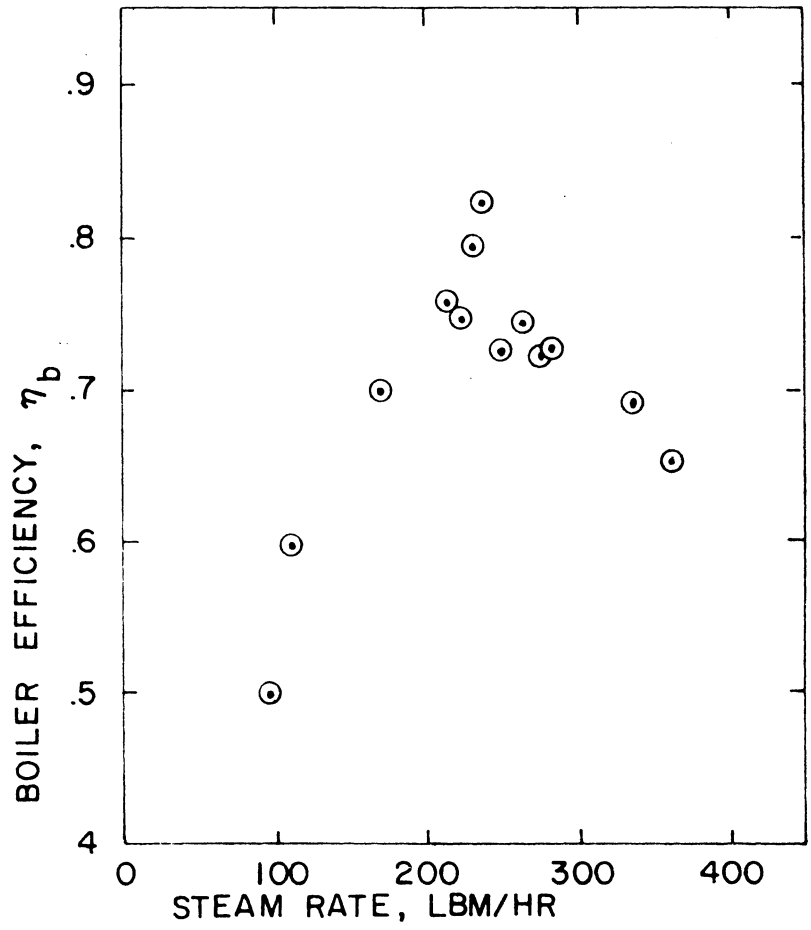

FIG. 6.6 TEST BOILER EFFICIENCY

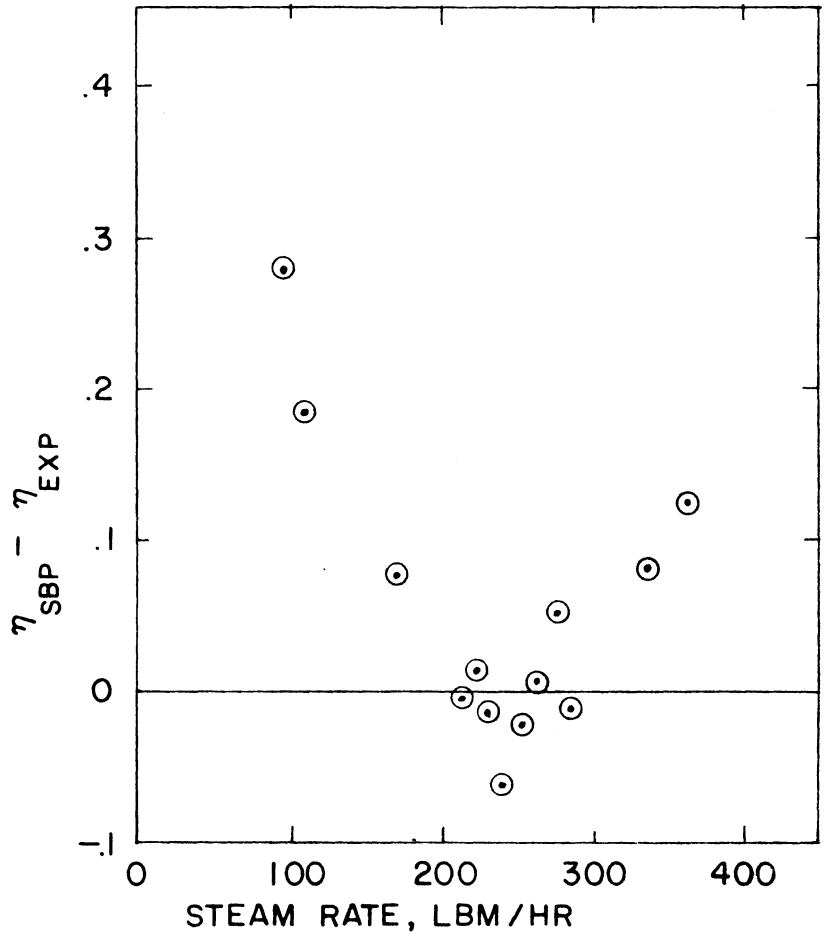

FIG. 6.7 DIFFERENCE BETWEEN PREDICTED AND MEASURED BOILER EFFICIENCY

of the burner gave no visual evidence of incomplete burning at low fuel rates.

In order to shed further light on the problem an energy balance has been performed on the test results. We may say that the heat loss through the casing walls is the difference between the enthalpy lost by the gas and the enthalpy gained by steam.

$$Q_{loss} = \Delta H_{gas} - \Delta H_{steam}$$

$$= m_g [HV_g - (h_{g_{flue}} - h_{g_{ambient}})] - m_s \Delta h_s$$

dividing by the total heating value of the fuel

$$m_f \cdot HV_f = m_g \cdot HV_g = m_g \frac{HV_f}{A/F + 1}$$

gives

$$\frac{Q_{loss}}{m_g \cdot HV_f} = 1 - (\frac{A}{F} + 1) \frac{h_{g_{fl}} - h_{g_{amb}}}{HV_f} - \frac{m_s \Delta h_s}{m_f HV_f}$$

Defining the first term as the loss fraction QLOSSF and noting that the last term is the boiler efficiency we have

$$QLOSSF = 1 - (\frac{A}{F} + 1) \frac{h_{g_{fl}} - h_{g_{amb}}}{HV_f} - \eta_b$$

which may be evaluated from test data.

The heat transfer through the casing walls, the so-called "radiation loss," is calculated by the program. The resulting QLOSSF ranges from 4.2% at minimum down to 1.9% at maximum load. These figures correlate

well with "radiation losses" from large boilers which have better insulation but more surface area per lbm of fuel burned. The difference between predicted and measured QLOSSF is plotted in Fig. 6.8. We note that this curve and that for boiler efficiency have the same shape. The minimum QLOSSF difference is in the 200-300 lbm/hr range. The large difference at higher loads may be explained by the low combustion efficiency already discussed. However, the maximum difference is at low loads--in fact for two cases the measured heat loss is greater than the predicted loss by an amount equal to over 20% of the heating value of the fuel! Another interpretation for these two points at low steam rates is that the actual heat loss is 6.8-8.5 times greater than the predicted value. But for the predicted values to be this much in error seems highly unlikely. In this heat transfer calculation the convective resistance on both sides is neglected since the insulation itself is the dominant resistance. Its thermal conductivity has been taken at 0.125 B/hr-ft-F which is on the high side even for an 1800°F mineral board. Thus it appears reasonable to expect the predicted heat loss to be high if anything.

The discussion above suggests the proposition that the experiment itself is the prime source of error. The first possibility is faulty instrumentation and observation. It is true that unshielded thermocouples and a fluctuating flow meter will introduce errors so a simple error analysis is in order. Boiler efficiency is

$$\eta_b = \frac{m_s (h_s - h_\ell)}{m_f \cdot HV_f}$$

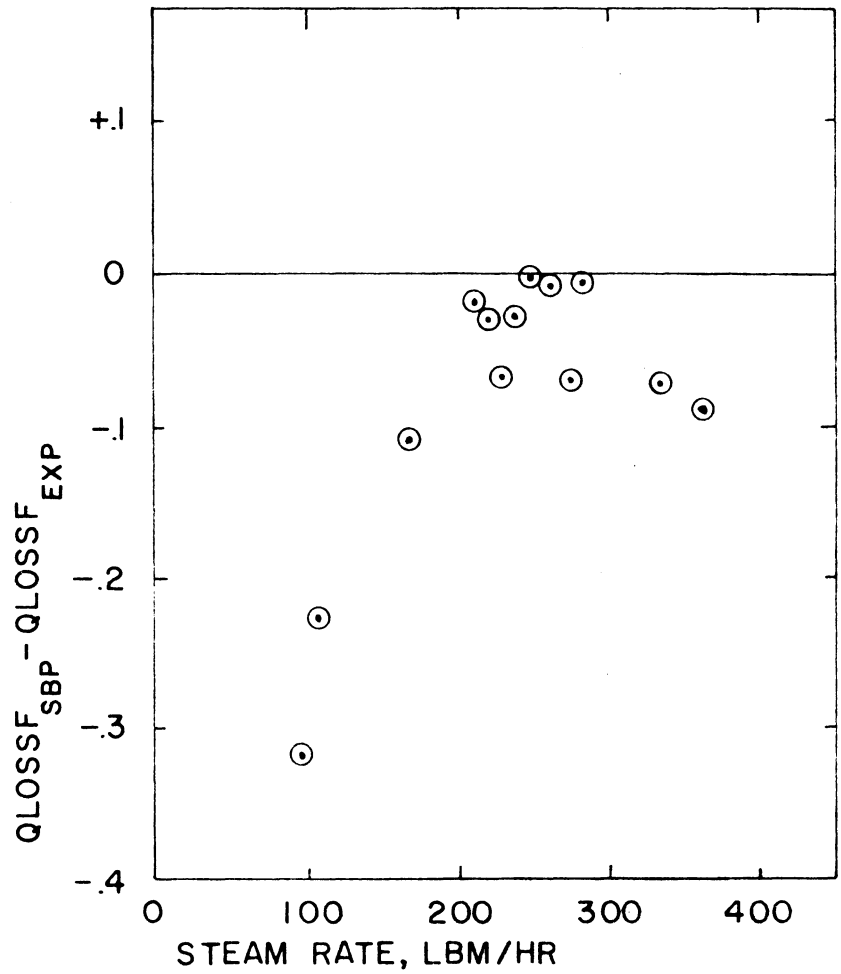

FIG. 6.8 DIFFERENCE BETWEEN PREDICTED AND MEASURED HEAT LOSS FRACTION

logarithmic differentiation gives

$$\frac{d\eta_b}{\eta_b} = \frac{d\ m_s}{m_s} + \frac{d(h_s - h_\ell)}{h_s - h_\ell} - \frac{d\ m_f}{m_f} - \frac{d\ HV_f}{HV_f}$$

$$= 0.040 + \frac{0.5(30)}{1200} - \frac{1.0(30)}{1200} - \frac{0.5}{100} - \frac{200}{18200}$$

$$= 0.040 + 0.0125 - 0.025 - 0.005 - 0.0111$$

where a 30°F temperature error has been assumed. The pressure error is far smaller (~ 5 psi) and has a smaller effect on enthalpy so it was ignored. The major uncertainty is in the water flow rate. Assuming a normal distribution of independent errors, the deviation in efficiency is

$$\frac{\text{dev } \eta_b}{\eta_b} = (0.040^2 + 0.0125^2 + 0.0250^2 + 0.005^2 + 0.0111^2)^{1/2}$$

$$= 0.0503$$

$$\text{dev } \eta_b = 0.0503\ \eta_b = 0.0503(0.75)$$

$$= 0.038$$

So the expected error in η_b is less than 4% whereas the difference between prediction and experiment rises to 28% at the minimum steam rate so the explanation does not lie here.

The other possibility is a malfunction of the equipment in some way. It was once proposed that the small fire at low load would reduce radiation in the combustion chamber. This would be an important

consideration at low load since under these conditions radiative heat transfer is 34% of the total while it is only 26% of the total at the highest load. However, if the radiation rate was down, less energy would be extracted from the gases and the flue temperature would be high. But the predicted and measured flue temperatures are in close agreement ($\pm$ 20°F) at low steam rates so this loss-of-radiation theory is unsupported.

It is known that there was a pin-hole water leak between the 3/8 and 1/2 in. tubes. This was only a few drops per minute initially and apparently had been plugged by small particles in the water by the time the final tests were run. A large water leak would have appeared as water dropping from the casing upon startup, i.e., before the boiler was hot enough to evaporate the leakage water into the gas stream.

In its final form the boiler had no external fuel leaks of any kind. The only remaining explanation is that the burner suffered from an internal "leak" in that some fuel went through the boiler without burning at low steam rates as well as at high. This does not seem probable but is suggested as a last resort!

One aspect of boiler performance which is not dependent on combustion efficiency is the water pressure drop as it flows through the boiler and turns to superheated steam. The measured values are given in Fig. 6.9 and are observed to approximately follow a parabolic dependence on flow rate. The scatter is due to varying steam conditions and an oscillating pressure gage on the boiler feed side despite the use of a three-plunger pump with a gas-over-water accumulator to

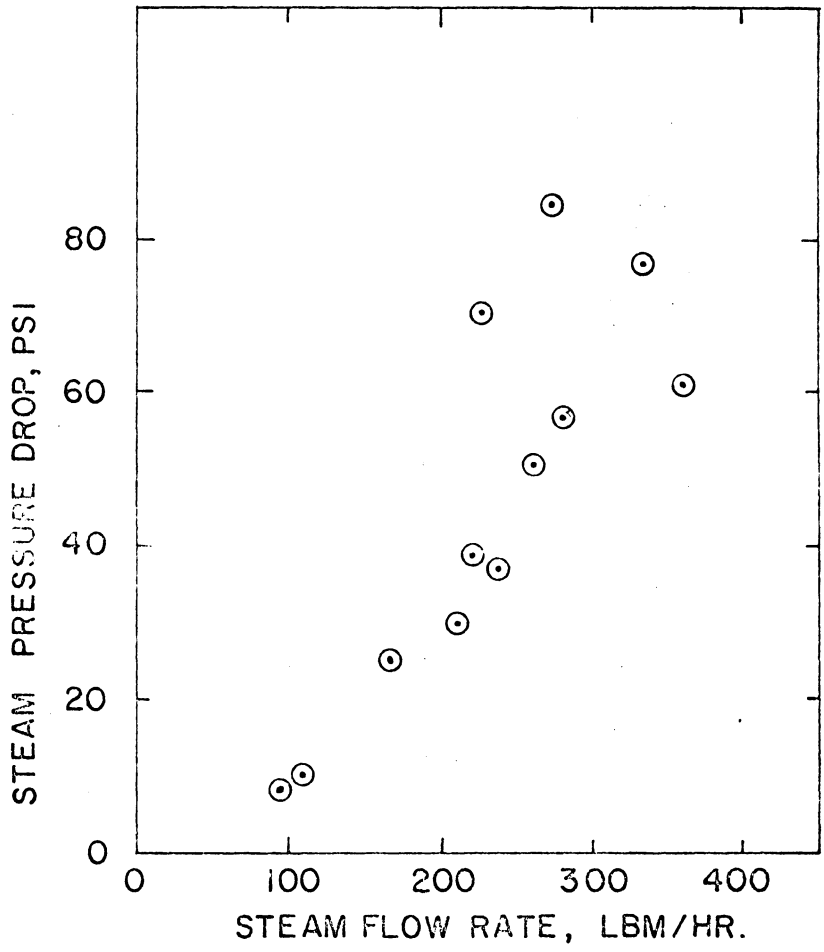

FIG. 6.9 WATER-SIDE PRESSURE DROP

reduce pulsations. The extremes of difference between predicted and measured values ranged from 10 to 58% with a mean of 30%. Thus it appears that the simple expression for pressure drop introduced in Sec. 3.4 would benefit from an increase in its coefficients.

VII. CONCLUSIONS AND RECOMMENDATIONS

The Transient Boiler Performance simulation has successfully passed the qualitative tests in the last chapter. It appears that the goal of developing a means of numerically testing control system algorithms has been reached. The simulation results do not agree well with the limited experimental data available over the full range of flow rate. Mid-range results do agree well, thereby validating the mathematical model, and post-test examination of the apparatus suggests equipment rather than simulation problems caused variations at the ends of the flow rate range. However, there are several areas where improvements can and will be made.

The mathematical model must be improved in the areas of steam properties and two-phase flow. At the earliest feasible date the ASME equations for thermodynamic and transport properties will be incorporated in the program. While the existing treatment of two-phase heat transfer and pressure drop leaves something to be desired, improvements in this area must await publication of a definitive analysis which pertains directly to a coil boiler.

The major disappointment with the program itself is the computer time required. About 30 minutes is needed to simulate a 17-coil boiler operating for 3 minutes of boiler time. The removal of extra printout and part of the iteration loop, in conjunction with the use of an optimizing two-pass compiler (Fortran IV), is expected to increase speed of execution by a factor of two.

Burner modifications to improve combustion efficiency are underway. These, plus data recording equipment, will permit reliable experimental data to be obtained in order to verify the program empirically.

VIII. SUMMARY

A steam generating unit consisting of a single tube heated by combustion gases has been modeled mathematically with emphasis on simulating non-steady behavior. The resulting digital computer program is particularly suited to predicting the response of automotive boilers to changes in operating conditions.

The heart of the model is the set of conservation laws for mass, momentum and energy of the steam. These are augmented with empirical relations for heat transfer and pressure drop plus steam table data. Allowance is also made for gas convection and radiation, heat loss to ambient, and energy storage in the tube wall. The resulting set of three partial differential equations in four unknowns is solved by removing specific volume derivatives from the set through substitution of steam table data in differential form. The differential equations are put in finite difference form which yields a set of quasi-linear algebraic relations which are solved on a digital computer. The program's predictions of non-steady performance have been qualitatively compared with experimental results found in the literature. A 12-in. diameter test boiler has been constructed and preliminary steady-state data from it are compared with the simulation.

REFERENCES

1. Bjerklie, J. W., and B. Sternlicht, "Critical Comparison of Low-Emission Otto and Rankine Engine for Automotive Use," SAE 69044.

2. Miner, S. S., "Developments in Automotive Steam Powerplants," SAE 690043.

3. Tabor, H., and L. Bronicki, "Establishing Criteria for Fluids for Small Vapor Turbines," SAE 931C, 1964.

4. Percival, W. H., "Flourochemical Vapor Machine," SAE 931B, 1964.

5. Bjerklie, J., and S. Luchter, "Rankine Cycle Working Fluid Selection and Specification Rationale," SAE 69063.

6. Doyle, E. F., T. LeFeuvre and R. J. Raymond, "Some Developments in Small Reciprocating Rankine-Cycle Engines Using Organic Working Fluids," SAE 700162.

7. Neil, E. B., "Thermodynamics of Vapor Powerplants for Motor Vehicles," SAE Transactions, April 1948, pp. 288-305.

8. Fraas, A. P., "Application of Modern Heat Transfer and Fluid Flow Experience to the Design of Boilers for Automotive Steam Powerplants," SAE 690047.

9. Doble, A., "The Use of Steam at High Temperatures and Pressures in Small Powerplants," Engine and Boiler House Review, 1937-8 (Reprinted in Doble Steam Cars, J. N. Walton, Light Steam Power, Isle of Man, U.K., approx. 1965).

10. Dooley, J. L., and A. F. Bell, "Description of Modern Automotive Steam Powerplant," SAE S338, 1962.

11. Garner, H. D., "Control of the Monotube Boiler," presented at the First Technical Meeting of the Steam Automobile Club of America, Oak Ridge, Tennessee, September 17, 1971.

12. Garner, H. D., "Critical Research Areas in Automotive Steam Engineering," The Steam Automobile, Vol. 10, No. 4.

13. Rossbach, R. J., "Space-Vehicle Rankine Cycle Power Plant Potassium-Turbine Development," ASME 63-WA-326.

14. Millman, V., "Advanced Technology Applied to a Steam Powered Vehicle," SAE 931A, 1964.

15. Kitrilakis, S. S., and E. F. Doyle, "The Development of Portable, Reciprocating Engine, Rankine Cycle Generating Sets," SAE 690046.

16. Snoke, D. R., and G. L. Mrava, "Silent Mercury Rankine Cycle Power System," SAE 883D, 1964.

17. Degner, V. R., and W. W. Velie, "Demonstration of a Self-Contained Organic Rankine Silent System," SAE 690062.

18. Lodwig, E., "Performance of a 35 hp Organic Rankine Cycle Exhaust Gas Powered System," SAE 700160.

19. Vickers, P. T., C. A. Amann, H. R. Mitchell and W. Cornelius, "The Design Features of the GM SE-101 - A Vapor-Cycle Powerplant," SAE 700163.

20. Fraas, A. P., "Control of Mobile Steam Powerplants," SAE 700118.

21. Maday, C. J., "A Dynamic Programming Approach to Stabilize Forced-Convection Two-Phase Flow System with "Pressure Drop Oscillations," ASME 69-HT-43.

22. "Selected Technology for the Electric Power Industry," NASA SP-5057, 1968.

23. Hess, H. L., J. R. Hooper and S. L. Organ, "Analytical and Experimental Study of the Dynamics of a Single Tube Counterflow Boiler," NASA CR-1230, 1969.

24. Fraas, A. P., and M. N. Ozisik, Heat Exchanger Design, Wiley, New York, 1965.

25. Peoples, J. A., Steam Automotive Analysis, Carlton Press, New York, 1970.

26. Richards, C. G., and H. D. Garner, "A Simplified Numerical Simulation of a Monotube Steam Boiler," Automatic Control Section, NASA-Langley, 1972, (unpublished).

27. Buis, J. P., "A Modified Serial Method for the Hybrid Solution of Hyperbolic Partial Differential Equations, and Its Application to the Simulation of a High-Pressure Forced-Flow Evaporator System," Laboratorium voor technische Natuurkunde, Technische Hogeschool Delft, Delft, the Netherlands, 1971.

28. Mayer, E. A., and G. W. Hurlong, "Steam Car Control Analysis," Quarterly Report No. 4, Project No. 2875, Bendix Corporation, Southfield, Michigan, 1972.

29. Adams, J., D. R. Clark, J. R. Louis, and J. P. Spanbauer, "Mathematical Modelling of Once-through Boiler Dynamics," IEEE Power Group Transactions, February 1965, pp. 146-156.

30. Livshits, M. A., B. N. Zolatarin, M. M. Chukvinskii, and G. I. Moseav, "Study of Pick-up of the PK-38 Once-Through Boiler in a Unit with the K-160-130 Turbine and its Operational Reliability with Sudden Changes in Load," Teploenergetika, 1966, Vol. 13, No. 3.

31. Krejsa, E. A., J. H. Goodykoontz, and G. H. Stevens, "Frequency Response of Forced-Flow Single-Tube Boiler," NASA TN D-4039, April 1967.

32. Kays, W. M., Convective Heat and Mass Transfer, McGraw-Hill, New York, 1966.

33. Rohsenow, W. M. (ed.), Developments in Heat Transfer, M.I.T. Press, Cambridge, Mass., 1964.

34. Tong, L. S., Boiling Heat Transfer and Two Phase Flow, Wiley, New York, 1966.

35. Peterson, J. R., "The Effect of Swirl Flow upon the Performance of Monotube Steam Generators," SAE 700116.

36. Kays, W. M. and A. L. London, Compact Heat Exchangers, National Press, Palo Alto, Calif., 1955.

37. Carnahan, Brice, H. A. Luther, and J. O. Wilkes, Applied Numerical Methods, Wiley, New York, 1969.

38. Ames, W. F., Numerical Methods for Partial Differential Equations, Barnes and Noble, New York, 1969.

39. Pierce, F. J., and W. F. Klinksiek, "An Implicit Numerical Solution of the Turbulent Three-Dimensional Incompressible Boundary Layer Equations," AD 728126, Virginia Polytechnic Institute and State University Report VPI-E-71-14, July 1971.

40. Gary, John, "On Certain Finite Difference Schemes for Hyperbolic Systems," Mathematics of Computation, January 1964, pp. 1-18.

41. Gourlay, A. R., and J. L. Morris, "Finite-Difference Methods for Non-Linear Hyperbolic Systems," Mathematics of Computation, January 1968, pp. 28-39.

42. von Rosenberg, D. U., Methods for the Numerical Solution of Partial Differential Equations, American Elsevier, New York, 1969.

43. Taylor, C. F., and E. S. Taylor, The Internal Combustion Engine, International Textbook, Scranton, Pa., 1948.

44. Marks, L. S., ed., Mechanical Engineers Handbook, McGraw-Hill, New York 1951.

45. Mooney, D. A., Mechanical Engineering Thermodynamics, Prentice-Hall, New York, 1953.

46. Keenan, J. H., and J. Kaye, Gas Tables, Wiley, New York, 1948.

47. Steam--Its Generation and Use, Babcock & Wilcox Company, New York, 1955.

48. Schnackel, H. C., "Formulations for the Thermodynamic Properties of Steam and Water," ASME Transactions, May 1958, pp. 959-966.

49. Steltz, W. G. and G. J. Silvestri, "The Formulation of Steam Properties for Digital Computer Application," ASME Transactions, May 1958, pp. 967-973.

50. Keenan, J. H., and F. G. Keyes, Thermodynamic Properties of Steam, Wiley, New York, 1936.

51. McAdams, W. H., Heat Transmission, McGraw-Hill, New York, 1954.

52. Combustion Engineering, Combustion Engineering--Superheater, Inc., New York, 1950.

53. Jakob, M., Heat Transfer, Wiley, New York, 1957.

APPENDIX A

THE DEPENDENCE OF ENGINE POWER ON CONDENSER TEMPERATURE

If we neglect second order effects like boiler feed pump work, heat transfer in the cylinder and mechanical friction, the enthalpy increase of the steam in the boiler, ΔH_s, is:

$$\Delta H_s = \Delta H_e + \Delta H_c$$

where ΔH_e and ΔH_c are the enthalpy drops in the engine and condenser.

The efficiency is defined as:

$$BTE = \frac{\Delta H_e}{\Delta H_s}$$

and an energy balance on the condenser gives

$$\Delta H_c = UA\ (TCOND - TAMB)$$

where UA is the product of condenser area and overall heat transfer coefficient and is assumed constant. These three equations may be combined:

$$\Delta H_e = \frac{\Delta H_e}{\Delta H_c}\ \Delta H_c$$

$$= \frac{BTE}{1-BTE}\ UA(TCOND - TAMB)$$

From this relation we could conclude that the engine power, which is proportional to ΔH_e, increases with increasing condenser temperature

TCOND. However, we know from both cycle analyses and test data that the brake thermal efficiency BTE will decrease with increasing TCOND with a resulting reduction in ΔH_e. Thus TCOND has opposing influences on the two factors which determine engine power. At extremes of TCOND either BTE or (TCOND - TAMB) go to zero hence ΔH_e is zero. Since ΔH_e is not zero for normal TCOND we know that for a given powerplant and operating conditions there is a TCOND that will maximize engine power. This result is shown in Fig. 1.2.

APPENDIX B

COMBUSTION GAS PROPERTIES

The fuel employed is diesel oil which may be approximated by the formula $C_{12}\ H_{26}$ having a lower heating value LHV = 18,200 B/lbm fuel (43). To assure complete combustion 10% excess air is used (44). Normal air may be taken to be 0_2 and N_2 in the ratio 1:3.76 by volume. The ideal combustion reaction is then:

$$C_{12}H_{26} + 1.1(18.5)\ (0_2 + 3.76N_2) \rightarrow 12CO_2 + 13H_2O + 1.1(18.5)3.76N_2 + \frac{18.5}{10}\ 0_2$$

For which the formula weights are:

$$170.2 + 2792 \rightarrow 528.0 + 234.2 + 2142 + 59.2$$

The air fuel ratio is $A/F = \frac{2792}{170.2} = 16.40$

If ambient air is at 85F and 70% relative humidity the absolute humidity is 124 grains H_2O/lbm dry air thus for one lbm-mole of fuel we induct

$$2792\ \frac{\text{lbm dry air}}{\text{mole fuel}}\ X\ \frac{124}{7000}\ \frac{\text{lbm } H_2O}{\text{lbm dry air}} = 49.5\ \frac{\text{lbm } H_2O \text{ inducted}}{\text{mole fuel}}$$

so the total mass of water in the flue gas is

$$234.2 + 49.5 = 283.7\ \frac{\text{lbm } H_2O}{\text{mole fuel}}$$

and the total mass of gas is

$$528.0 + 283.7 + 2142 + 59.2 = 3013 \frac{\text{lbm flue gas}}{\text{lbm mole fuel}}$$

thus the mass fractions are:

	f_i
O_2	0.0196
N_2	.7115
H_2O	.0942
CO_2	.1752

The specific heat may be calculated from

$$c_p = \sum_{i=1}^{n} f_i \, c_{p_i}$$

and the enthalpy from

$$h = \sum_{i=1}^{n} f_i \, h_i \qquad \text{(Ref. 45)}$$

where the constituent data come from (46).

Thermal Conductivity and Viscosity

Conductivity k is for fuel oil with 15% excess air (data for 10% excess air was not found).

Viscosity is for "average flue gas" (47).

T, °F	0	500	1000	1500	2000	2500	3000
k, $\frac{B}{hr\text{-}ft\text{-}F}$		.0220	.0290	.0360	.0430	.0490	
μ, $\frac{lbm}{ft\ hr}$	.0365	.0630	.0830	.1010	.1168	.1309	.1420

Gas Constant

$$R = \sum f_i R_i = R_u \sum \frac{f_i}{MW_i}$$

$$= 1545 \left(\frac{0.0196}{32} + \frac{0.7115}{28.016} + \frac{0.0942}{18.016} + \frac{0.1752}{44.01}\right)$$

$$= 54.35 \text{ ft } lb_f/lbm\ °R$$

These properties are plotted in Fig. B-1 and Fig. B-2. To facilitate adaptation to the computer these curves have been fitted with polynomials which are given below with their maximum error.

$$h = 0.1129033(10)^3 + 0.2652727\ T + 0.1390926(10)^{-4}\ T^2$$

residual 3.4 B/lbm

$$T = -0.4143591(10)^3 + 0.3769359(10)^1\ h - 0.4481329(10)^{-3}\ h^2$$

residual 16.4 °F

$$c_p = 0.2550812 + 0.4023570(10)^{-4}\ T - 0.9408869(10)^{-9}\ T^2 - 0.8431375(10)^{-12}\ T^3,\ B/lbm\ F,\ error = 0.8\%$$

$$\mu = 0.3632385(10) + 0.5439683(10)^{-4}\ T - 0.8065211(10)^{-8}\ T^2 + 0.5337830(10)^{-12}\ T^3,\ lbm/ft\text{-}hr,\ error = 2.2\%$$

$$P_r^{2/3} = 0.7882808 + 0.2263911(10)^{-3}\ T - 0.1580168(10)^{-6}\ T^2 + 0.5023598(10)^{-10}\ T^3 - 0.5769971(10)^{-14}\ T^4,\ error\ 0.9\%.$$

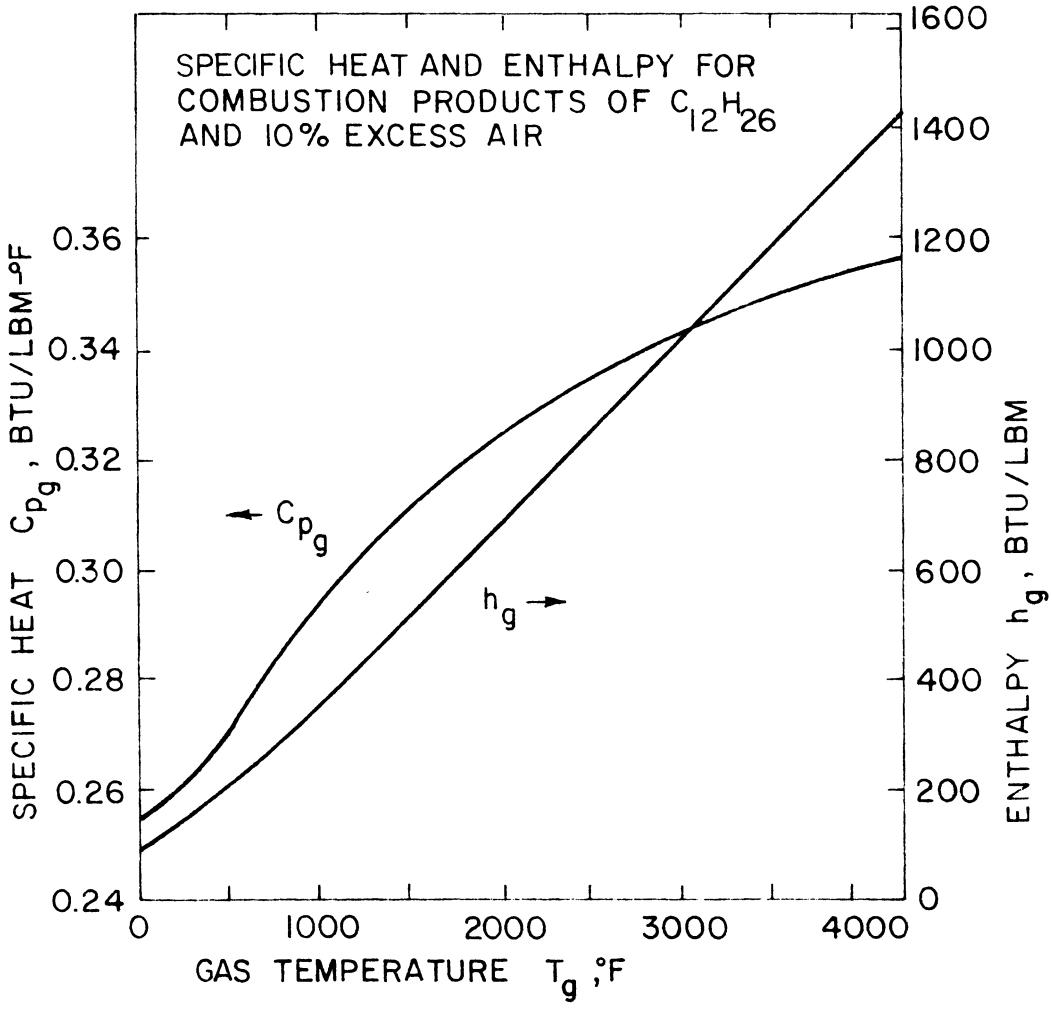

FIG. B.1 ENTHALPY AND SPECIFIC HEAT OF FLUE GAS

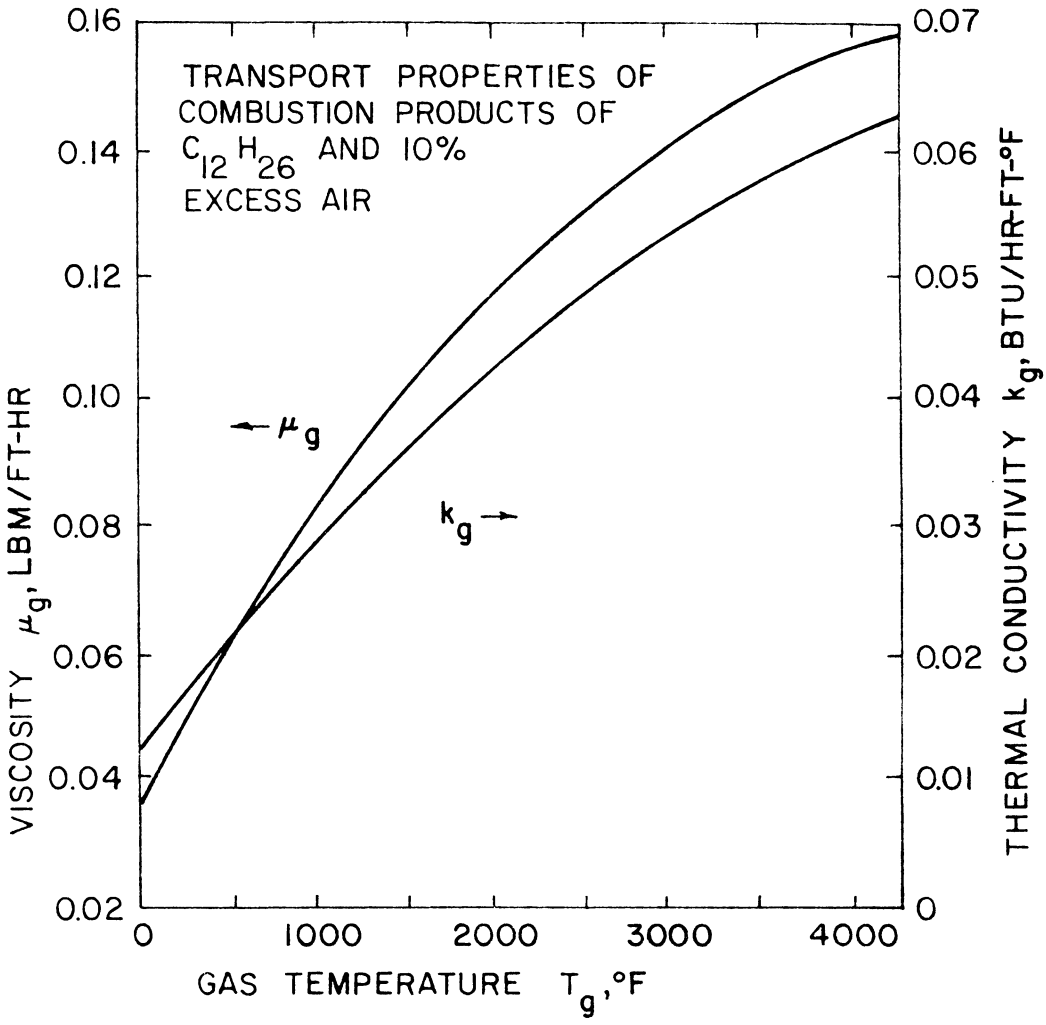

FIG. B.2 TRANSPORT PROPERTIES OF FLUE GAS

Adiabatic gas enthalpy and flame temperature

The heating value of the flue gas is

$$HVG = \frac{18200}{A/F + 1} \text{ B/lbm gas} \tag{B.1}$$

The gas enthalpy after adiabatic combustion is

$$h_{ad} = h_{amb} + HVG \tag{B.2}$$

To relate the enthalpy of the gas leaving the combustion chamber h_{cc} to the gas temperature T_{cc} we use two linear approximations. In the 1600-3200 F range Fig. B.1 may be used to derive

$$h_{cc} = 34 + 0.336\ T_{cc} \tag{B.3}$$

and from Fig. D.2 we obtain the radiant heat flux as

$$q_r = 6900 + 6.2\ T_{cc} \tag{B.4}$$

We may also write the energy balance

heat radiated from combustion chamber = enthalpy drop of gas

or

$$q_r\ A_r = m_g(h_{ad} - h_{cc}) \tag{B.5}$$

Substituting (B.3) and (B.4) in (B.5) and solving for T_{cc} gives

$$T_{cc} = \frac{h_{ad} - 34 + 6900\ \frac{A_r}{m_g}}{0.336 + 6.2\ \frac{A_r}{m_g}} \tag{B.6}$$

For a given boiler and operating condition A_r, m_g, T_{amb} and A/F are known. The computer uses equations (B.1), (B.2) and (B.6) to calculate T_{cc}.

APPENDIX C

STEAM PROPERTIES

The thermodynamic properties of steam are curve fits (48,49) to Kennan and Keyes (50). These were chosen in preference to the equations given in the 1967 ASME Steam Tables because they were simpler and therefore less demanding of computer time. These two sources have been compared with the result that the maximum error in enthalpy is 2.0 Btu/lbm in the pressure range 400-1600 psi and the temperature range from saturation to 1200 F. This difference does not significantly change the results given. In any case, the ASME tables can be programmed and substituted if desired.

Viscosity, conductivity and Prandtl number have been approximated with simple curve fits with an error generally within 5% but as high as 37% for one point on the saturated vapor line. These relations are presented below but it is recommended that the ASME equations be used for far greater accuracy at a modest increase in complexity.

$$\mu_\ell = \frac{1}{0.00833\ T - 0.225}$$

$$k_\ell = 0.322 + 5.54(10)^{-4}T - 9.835(10)^{-7}T^2$$

$$P_{r_\ell} = 10.4 - 0.09349\ T + 3.388(10)^{-4}T^2 - 5.523(10)^{-7}T^3 + 3.366(10)^{-10}T^4$$

$$\mu_v = 0.122 - (5.54(10)^{-5} - 1.96(10)^{-9}p)(1885 - T)$$

$$k_v = -0.0084 + 2.036(10)^{-6} p + 4.652(10)^{-5} T + \frac{3.817}{T - 0.246\,p}$$

$$P_{r_v} = 0.523 - 5.079(10)^{-5}\, p + 1.585(10)^{-4} T + \frac{214}{T - 0.246\,p}$$

where the units are the same as for the gas properties.

The specific volume derivatives $\left.\frac{\partial v}{\partial h}\right|_p$ and $\left.\frac{\partial v}{\partial p}\right|_h$ are needed in order to introduce the equation of state into the continuity equation. They cannot be evaluated directly from steam tables but we can calculate them indirectly. In the one-phase region we may write

$$v = f(p,T)$$

$$h = f(p,T)$$

or taking total differentials

$$dv = \left.\frac{\partial v}{\partial p}\right|_T dp + \left.\frac{\partial v}{\partial T}\right|_p dT \qquad (C.1)$$

$$dh = \left.\frac{\partial h}{\partial p}\right|_T dp + \left.\frac{\partial h}{\partial T}\right|_p dT \qquad (C.2)$$

For dp = 0 we divide (C.1) by (C.2) to get

$$\left.\frac{\partial v}{\partial h}\right|_p = \frac{\left.\frac{\partial v}{\partial T}\right|_p}{\left.\frac{\partial h}{\partial T}\right|_p} \qquad (C.3)$$

We can also set dh = 0, solve (C.2) for dT, and substitute it in (C.1) to obtain

$$\left.\frac{\partial v}{\partial p}\right|_h = \left.\frac{\partial v}{\partial p}\right|_T - \frac{\left.\frac{\partial v}{\partial T}\right|_p}{\left.\frac{\partial h}{\partial T}\right|_p} \left.\frac{\partial h}{\partial p}\right|_T$$

or after substituting (C.3)

$$\left.\frac{\partial v}{\partial p}\right|_h = \left.\frac{\partial v}{\partial p}\right|_T - \left.\frac{\partial v}{\partial h}\right|_p \left.\frac{\partial h}{\partial p}\right|_T \tag{C.4}$$

For the two-phase region we write

$$v = x\, v_g + (1-x)\, v_f$$

$$h = x\, h_g + (1-x)\, h_f$$

taking total derivatives

$$dv = x\, dv_g + v_g\, dx + (1-x)dv_f - v_f dx$$

$$dh = x\, dh_g + h_g\, dx + (1-x)\, dh_f - h_f\, dx$$

But v_g, v_f, h_g, h_f are functions of pressure only so $dv_g = \frac{dv_g}{dp}\, dp$, etc. Substituting these relations gives

$$dv = \left[x \frac{dv_g}{dp} + (1-x) \frac{dv_f}{dp}\right] dp + [v_g - v_f]\, dx \tag{C.5}$$

$$dh = \left[x \frac{dh_g}{dp} + (1-x) \frac{dh_f}{dp}\right] dp + [h_g - h_f]\, dx \tag{C.6}$$

For dp = 0 divide (C.5) by (C.6) to get

APPENDIX D

RADIATION FROM COMBUSTION CHAMBER

The determination of radiation from flames in largely empirical. The major uncertainty is the flame intensity where we are concerned not only with flame size, temperature and overall composition but with the detailed specification of the size spectrum of the solid particles which make the flame luminous. We start with some overall correlations.

Orrok-Hudson (51)

This correlation was probably based on data from large coal furnaces.

$$\frac{q_{\text{radiation}}}{q_{\text{total released}}} = \left[1 + \frac{A/F}{27} \sqrt{\frac{m_{\text{coal, lbm/hr}}}{A_{\text{radiation, ft}}}} \right]^{-1}$$

For coal with a heating value HV = 11,600 B/lbm and air fuel ratio A/F = 11.0

$$\frac{q_r}{q_t} = \left[1 + \frac{11}{27} \sqrt{\frac{q_t/1000}{11600/1000}} \right]^{-1} = \frac{1}{1 + 0.1195 \sqrt{q_t, \text{ kB/hr-ft}^2}}$$

Combustion Engineering (52)

This data is for large furnaces with clean water walls (slag-free water tubes facing the furnace).

The two sources above give the data plotted in Fig. D-1.

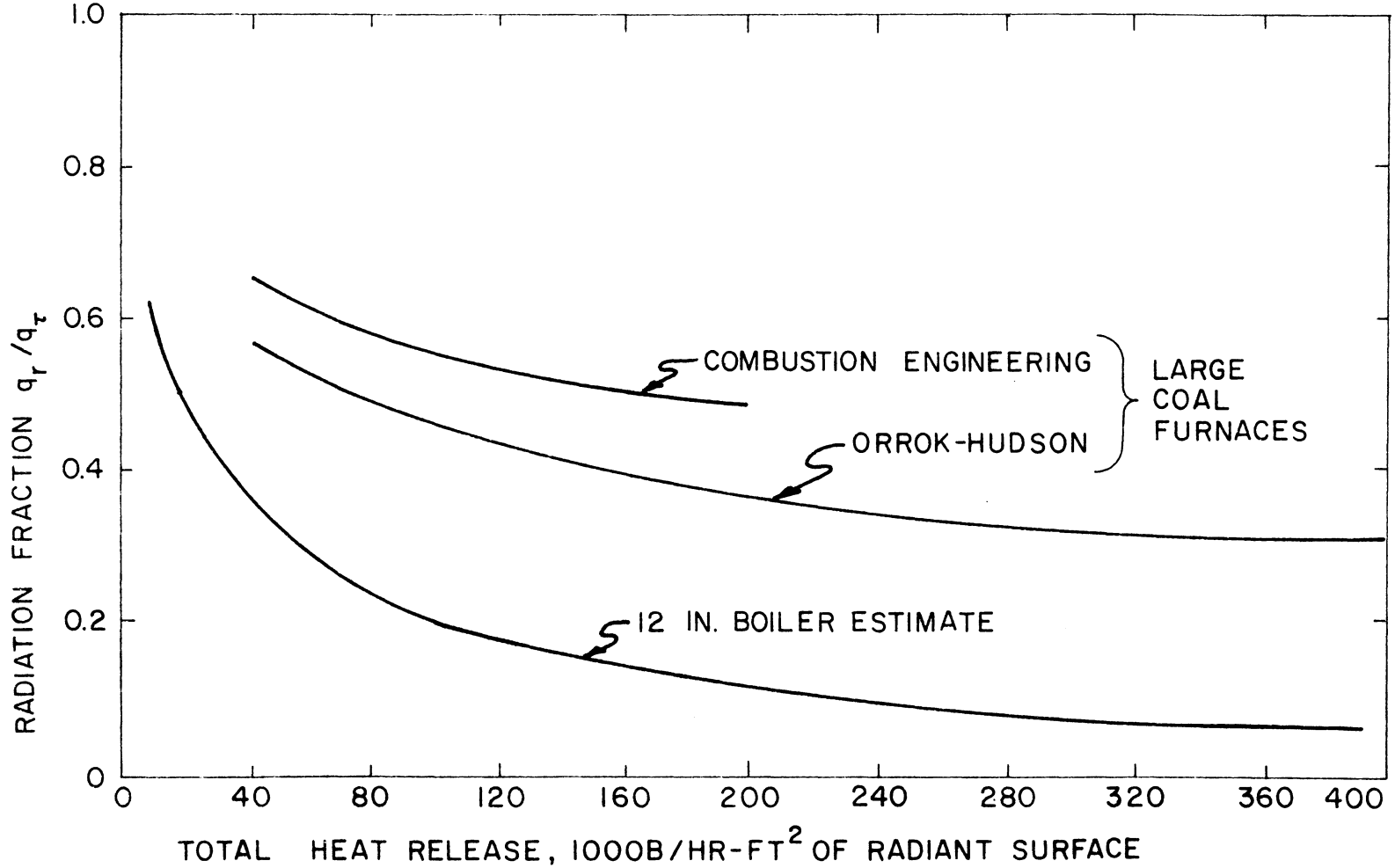

FIG. D.1 RADIATION FRACTION VS TOTAL HEAT RELEASE

Combustion Chamber Temperature From Radiation Laws

From a heat balance

$$q_{total} = q_{out} + q_{radiated}$$

where q_{out} is the heat flux leaving the combustion chamber (cc) by convection. If there are no significant temperature gradients in the cc itself (probably a good assumption in flame proper, i.e., away from walls) the above equation may be written

$$\frac{q_r}{q_t} = 1 - \frac{q_o}{q_t} = 1 - \frac{h_{cc} - h_{amb}}{HVG}$$

In this way the radiation fraction q_r/q_t may be related to the flame temperature T_{cc}. For T_{cc} = 2000 F we get, e.g.,

$$\frac{q_r}{q_t} = 1 - \frac{700 - 134}{1110} = 0.490$$

Radiation from Non-luminous Gases - From Jakob (53)

Water and carbon dioxide are the only constituents in the flue gas which radiate significantly. For a given total pressure of one atmosphere the emissivity ε and absorbitivity α depend on the gas temperature T_g, partial pressure P_p and mean beam length L (a characteristic size of the combustion chamber).

For a cylinder of equal length and diameter L = 0.6D so for the 12 in. boiler we estimate:

$$L = 0.6\,\frac{D+L}{2} = 0.6\,\frac{11+15}{2(12)} = 0.65 \text{ ft.}$$

For the combustion of $C_{12}H_{26}$ with 10% excess air, the partial pressures are:

$$P_c = \frac{\text{moles } CO_2}{\text{total moles}} (P_{TOT}) = \frac{12}{103.35} (1 \text{ atm}) = 0.116 \text{ atm}$$

$$P_w = \frac{\text{mole } H_2O}{\text{total mole}} (P_{TOT}) = \frac{12}{103.35} (1) = 0.126 \text{ atm}$$

The pressure-length product is

$P_cL = 0.65\ (0.116) = 0.0754$ atm-ft — use 0.08 atm line on charts in Jacob

$P_wL = 0.65\ (0.126) = 0.0819$ atm-ft

The gas emissivity decreases with temperature since the density is reduced.

For CO_2 at $P_T = 1$ atm the correction factor for CO_2 is $C_c = 1.0$ and for water with $\frac{1}{2}(p_T + p_w) = \frac{1}{2}(1.0 + 0.126) + 0.563$ atm

The correction factor $c_w = 1.09$

When both gases are present the total emissivity must be reduced.

For $\frac{p_w}{p_c + p_w} = \frac{0.126}{0.116+0.126} = 0.52$, $\Delta\varepsilon = 0.$

So the total gas emissivity is

$$\varepsilon_g = \varepsilon_c C_c + \varepsilon_w C_w - \Delta\varepsilon$$

$$= \varepsilon_c + 1.09\ \varepsilon_w$$

Now we consider the gas absorbtivity α_g

For $T_g/T_t > 1.25$ we can approximate α_g within 10% with

$$\alpha_g = \varepsilon_t = (\varepsilon_c + \varepsilon_w C_w)_t$$

where the emissivities are evaluated at T_t.

Thus the net radiative transfer flux is

$$q = \varepsilon_e \sigma(\varepsilon_g T_g^4 - \varepsilon_t T_t^4)$$

Since the tube surface temperature T_t is a maximum of only 80 F above the steam temperature (SBP results) we neglect the heat flux radiated back from the tube leaving

$$q_r = \varepsilon_e \sigma \varepsilon_g T_g^4$$

From the data plotted in Jakob we calculate the gas emissivity ε_g, the radiation flux q_r, and plot them in Fig. D.2.

We note that q_r varies more slowly than T_g^4 since ε_g falls with temperature--in fact q_r is linear with T_g for 1600 F < T_g < 3200 F. The 12 in. boiler under consideration has a certain radiation surface based on the area of a cylinder that would just fit in the combustion chamber. However, the effective surface is larger by a factor of about 1.4 due to the curvature or corrugations of the cc wall formed by the round tubes.

This heat radiated from non-luminous gases represents the lower limit of heat transferred from the combustion chamber. In reality an atomized oil flame is highly luminous which increases the heat flux

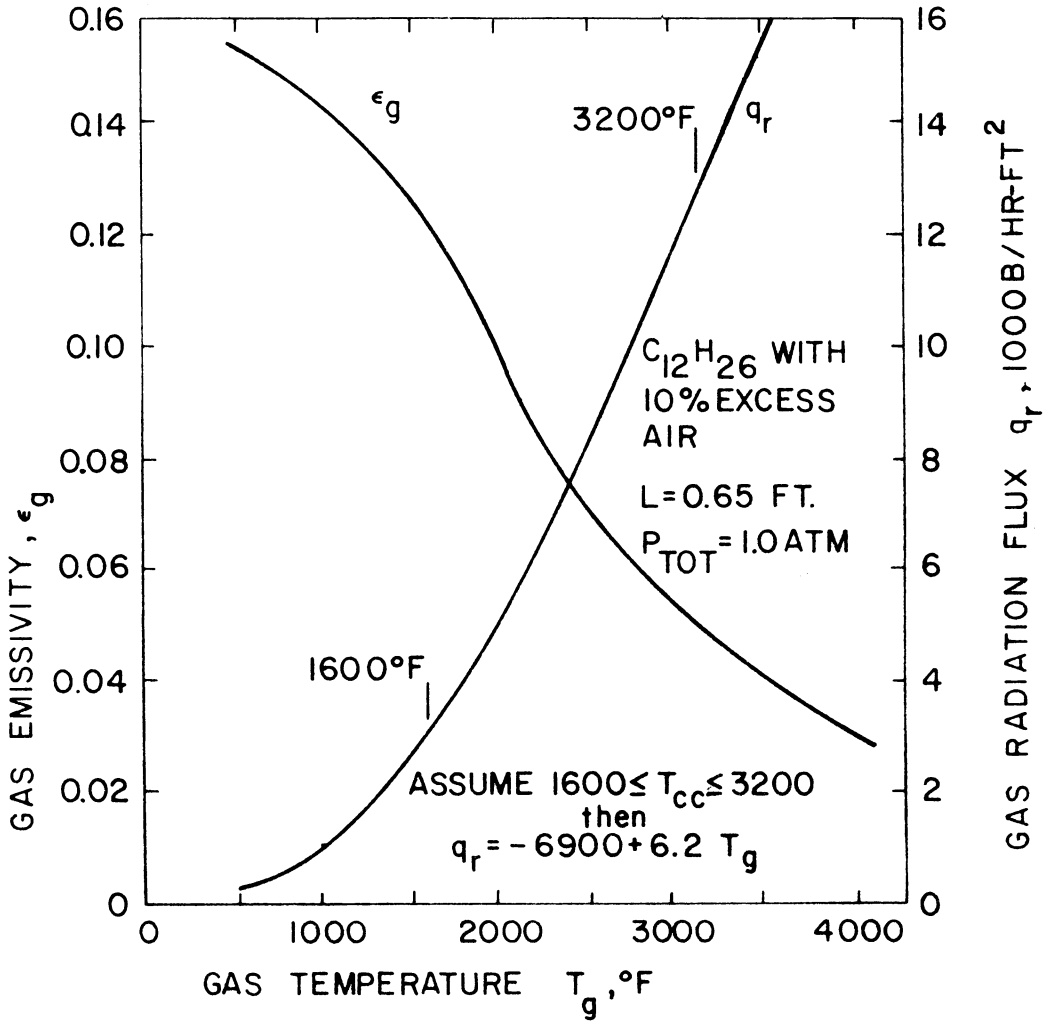

FIG. D.2 EMISSIVITY AND RADIANT HEAT FLUX OF FLUE GAS

"often by more than 100%", Jakob. McAdams (51) quotes instances where luminosity increased the heat flux by a factor of 3 (natural gas) or 4 (acetylene). The non-luminous radiation fraction based on the above is also plotted on Fig. D-1.

In the absence of a good correlation for luminous flames we will double the radiation flux based on the above information.

APPENDIX E

USAGE OF COMPUTER PROGRAM

The TBP simulation consists of a main program and four subroutines. It is written in FORTRAN IV and all calculations are performed in double precision. This latter feature could be limited to a small class of calculations in which roundoff error is unusually important with the attendant benefit of reduced computer time. No special setups such as disks, tapes or special library functions are required. It has run on an IBM 370 and a Xerox Sigma 6 with no changes at all to the program.

The subroutines and their functions are:

GAST - calculates gas properties per Appendix B. Radiation in the combustion chamber is computed following Appendix D hence the program is currently set up for small boilers; i.e., the characteristic length of the combustion chamber (cc) is 0.65 ft. If the cc is larger or the flame more luminous, the simulated radiation will be less than it should be.

STEAMT - This provides steam table data as described in Appendix C.

TRITRI - This algorithm solves the set of matrix equations resulting from the finite difference approximations to the general differential equations (Chapter IV).

CONTRL - This is the control center for the entire simulation. It is programmed by the user to vary the boundary conditions as desired. Through COMMON statements the following variables are available and may be varied at will:

TIM = time, sec

DTIM = step size, sec

TSTOP = maximum TIM, case is completed when TIM = TSTOP

DTP = printout interval, sec

WDS = weight flow rate of feed water, lbm/hr

WDG = weight flow rate of gas, lbm/hr

AVAT = area ratio of throttle valve to final tube setment

PS(j), VS(j), HS(j), US(j), TS(j) — steam pressure, psia; specific volume ft^3/lbm; enthalpy, B/lbm; velocity, ft/sec; and temperature, F at all tube stations j.

A READ or WRITE statement could be added if desired.

Data cards provide boiler details and initial conditions for the program. In the order read-in they are:

1. Instruction Card - determines what data is to be read in - Format (3I1).

   Column

   1 KCNFIG = 1 to read in a new configuration (card 2)

   2 KCOIL = 1 to read new coil data (card 3)

   3 KBNDRY = 1 to read new boundary (actually initial) conditions (card 4)

An instruction card must precede every case. If zero (0) is placed in any column the corresponding data will not be read, and the old data read in for an earlier case will be used.

2. Configuration Card - Format (12F6.0)

1-6	DCO	= outside diameter of coils, in. DCO is 12 in. in Fig. 5.1.
7-12	DCI	= inside diameter of spiral coils, in
13-18	DGIN	= diameter of firetube leading to combustion chamber, in. DGIN = DCI in the boiler considered here.
19-24	DGOUT	= diameter of flue gas exit from cool end of boiler casing, in.
25-30	AIRFUL	= Air/Fuel ratio on mass basis

3. Coil Cards - Format (12F6.0)

1-6	DTO	= outside diameter of boiler tube, in
7-12	FRAD	= fraction of radiation from cc that strikes coil
13-18	XT	= ratio of tube spacing transverse to gas flow to DTO
19-24	XL	= ratio of tube spacing longitudinal to gas flow to DTO
25-30	TWL	= tube wall thickness, in
31-26	CONDT	= thermal conductivity of tube, B/hr ft F
37-42	CPT	= specific heat of tube, B/lbm F

One coil card is read for each spiral coil. The closely wound helical coil and the final spiral from which the steam leaves the boiler may be broken down into as many "coils" as desired within the present limit of 26 coils total (set by DIMENSION statements). A blank or zero card should follow the last coil card to signify the end of the coil cards and permit the program to evaluate the number of coils NC.

All data above are printed at the top of the output sheet.

4. Boundary Cards

First Boundary Card - Format (12F6.0)

1-6	WDS	= feed water flow rate, lbm/hr
7-12	WDG	= combustion gas flow rate, lbm/hr
13-18	TIM	= initial time, sec

Second Boundary Card - Format (10F8.0)

1-8	TG	= gas temperature, F
9-16	TTO	= temperature of outside of tube, F
17-24	TTC	= temperature of midpoint of tube wall, F
25-30	TTI	= temperature of inside surface of tube, F
31-36	TS	= steam temperature, F
37-42	PS	= steam pressure, psia
43-48	VS	= steam specific volume, ft^3/lbm
49-54	HS	= steam enthalpy, B/lbm
55-60	US	= steam velocity, fps

If there are N coils the program will read N + 1 of these Second Boundary Cards. However, if a zero (blank) card is encountered before N + 1 cards are read, the remaining stations will be given the same initial conditions as the last station read. This latter feature is convenient for a cold start where all the temperature are the same and pressure drops small.

The constants which are built into the program are:

TAM	= ambient air temp. = 85 F
RHOT	= tube density = 490 lbm/ft^3 (steel)
DTIMMN	= minimum step size = 0.001 sec

CRCH = step size constant C = 500

Every DTP sec. the following is printed:

TIM = time, sec

DTIM = time step size, sec

RCH = relative change (R) in state

NSTEP = number of integration steps since start of simulation

In addition to the line above the properties below are printed for each station j.

J = station number starting at cold end of tube

TG = gas temperature, F

TTO = outside tube temperature, F

TTC = center of tube wall temperature, F

TTI = inside tube temperature, F

TS = steam temperature, F

PS = steam pressure, psia

X = steam quality

VS = steam specific volume, ft^3/lbm

HS = steam enthalpy, B/lbm

US = steam velocity, fps

WDSJ = steam flow rate, lbm/hr

BAL1 = normalized error fraction in mass equation

BAL2 = normalized error fraction in momentum equations

QVWW = heat transfer/volume, B/hr-ft^3

BAL3 = normalized error fraction in energy equation

VSER = normalized error in specific volume computed from derivatives relative to specific volume from steam tables.

COMPUTER PROGRAM

```
C          TRANSIENT BOILER PERFORMANCE NO 3
      IMPLICIT REAL*8(A-H,O-Z)
      COMMON /TRI1  / US(28),PS(28),HS(28),ATRI(9,27),
     1BTRI(9,27),CTRI(9,27),DTRI(3,27),NC
      COMMON /CNTRL1/TIM,DTIM,TP,DTP,TSTOP,WDS,WDG,AVAT,
     1VS(27),X(27),TS(27),NSTEP,KCH
      DIMENSION USN(28),PSN(28),HSN(28),TSN(27),VSN(27),
     1VSD(27)
      DIMENSION DVHP (27),DVPH (27),DVHPN(27),DVPHN(27),
     1DVPHB(27),TG(27),TGN(27),     YG(27),YS(27),XN(27),
     2DVHPB(27),HG(27),HGN(27)
      DIMENSION QVW(27),DPSXW(27),USBW(27),VSBW(27),REW(27)
      DIMENSION DTO(26),ERAD(26),XT(26),XL(26),TWL(26),
     1 CPT(26),CONDT(26)
      DIMENSION DTI(26),DHYD(26),AHT(26),AFLS(26),AFLG(26),
     1WTT(26),CDPV(26),CUG(26),CFG(26),CUL(26),CUV(26),
     2 ZT(26),ARS(27),ALOSS(26),CFV(26),YT(26)
      DIMENSION TTO(27),TTCN(27),TTC(27),TTCN(27),TTI(27),
     1CTAD(27)          ,CT1(27),CT2(27),CT3(27),CT4(27),
     2TTIN(27)
      PI=3.14159
      GC=32.17
      CJ=778.16
      CGJ=GC*CJ
      CGJ2=CGJ*2.
      TAM=85.
      CALL GAST(TAM,ARWG,HGAD,HGAM,C,V,P,2)
      RHOT=490.
      ARS(1)=1.
      DTIMMN=0.0010
C          READ DATA
    2 READ(5,13)KCNFIG,KCOIL,KBNDRY
```

```
13    FORMAT(6I1)
      IF(KCNFIG+KCOIL+KBNDRY.EQ.0) STOP
      IF(KCNFIG.EQ.0) GO TO 17
      READ(5,1)DCO,DCI,DGIN,DGOUT,AIRFUL
1     FORMAT(12F6.0)
      AF=PI/4.*(DCO**2-DCI**2)/144.
      AGIN2=(PI/4.*(DGIN /12.)**2)**2
      AGOUT2=(PI/4.*(DGOUT/12.)**2)**2
      HVG=18200./(AIRFUL+1.)
      HGAD=HGAM+HVG
      WRITE(6,14)DCO,DCI,DGIN,DGOUT,AIRFUL
14    FORMAT( /'      DCO      DCI     DGIN    DGOUT   AIRFUL'
     1 /4F8.3,F8.2/)
17    IF(KCOIL.EQ.0) GO TO 15
      WRITE(6,24)
24    FORMAT(     '  I      DTO     FRAD       XT       XL     '
     1'TWL    CONDT      CPT       UT       ZT      AHT     AHTN'
     2'    ALOSS      WTT   WTTTOT')
      ARAD=0.
      ACCLOS=0.
      AHTN=0.
      WTTTOT=0.
      DO 12 J=1,26
      READ(5,1)DTO(J),FRAD(J),XT(J),XL(J),TWL(J),CONDT(J),
     1CPT(J)
      IF(DTO(J).EQ.0.) GO TO 19
      NC=J
      NC1=NC+1
      NC2=NC+2
      ENCH=2*NC
      ZT(J)=AF/(XT(J)*DTO(J)/12.)
      IF(XT(J).LT.0.) ZT(J)=-XT(J)
```

```
      AHT(J)=PI*DTO(J)/12.*ZT(J)
      ARAD=ARAD+FRAD(J)*AHT(J)
      ALOSS(J)=PI*DCO*DTO(J)*XL(J)/144.
      IF(XT(J).LT.0.) ALOSS(J)=DTO(J)/12.*ZT(J)
      IF(XT(J).LT.0.) ACCLOS=ACCLOS+ALOSS(J)
      AHTN=AHTN+AHT(J)
      YT(J)=CONDT(J)/TWL(J)*12.
      WTT(J)=PI*(DTO(J)-TWL(J))*TWL(J)*ZT(J)*RHOT/144.
      WTTTOT=WTTTOT+WTT(J)
12    WRITE(6,26)J,DTO(J),FRAD(J),XT(J),XL(J),TWL(J),
     1CONDT(J),CPT(J),YT(J),ZT(J),AHT(J),AHTN,ALOSS(J),
     2WTT(J),WTTTOT
26    FORMAT(I3,5F8.3,F8.1,F8.3,F8.0,6F8.2)
19    DO 27 J=1,NC
      DTO(J)=DTO(J)/12.
      TWL(J)=TWL(J)/12.
      DTI(J)=DTO(J)-2.*TWL(J)
      AFLS(J)=PI/4.*DTI(J)**2
      I1=J-1
      IF(J.EQ.1) I1=1
      ARS(J+1)=AFLS(I1)/AFLS(J)
      FCURV=(2.*DTI(J)**2/((DCO-DTO(J))**2+(DCI+DTO(J))**2))
     1**0.05
      IF(XT(J).LT.0.) FCURV=(DTI(J)/(DCO-DTO(J)))**0.1
      CUV(J)=0.0210*FCURV/DTI(J)
      CUL(J)=0.0155*FCURV/DTI(J)
      CFV(J)=0.184*FCURV
      CTAD(J)=CONDT(J)/(RHOT  *CPT(J)*(TWL(J)/2.)**2*3600.)
      CT1(J)=(1.+TWL(J)/(2.*DTO(J)))*TWL(J)/(2.*CONDT(J))
      CT2(J)=1.+TWL(J)/(DTI(J)+DTO(J))
      CT3(J)=1.-TWL(J)/(DTI(J)+DTO(J))
      CT4(J)=(1.-TWL(J)/(2.*DTI(J)))*TWL(J)/(2.*CONDT(J))
```

```
      IF(XT(J).LT.0.) GO TO 27
      AFLGT=AF*(XT(J)-1.)/XT(J)
      AFLGD=AF*(DSQRT(XT(J)**2+4.*XL(J)**2)-2.)/XT(J)
      AFLG(J)=DMIN1(AFLGT,AFLGD)
      DHYD(J)=4./PI*XL(J)*(XT(J)-1.)*DTO(J)
      CUG(J)=0.0574*(XL(J)+6.5)*DSQRT(XT(J)-1.)
      CEG(J)=0.181*PI*(XL(J)+1.)*(XT(J)-0.86)/(XT(J)-1.)
   27 CDPV(J)=ZT(J)/(144.*2.*GC*DTI(J))
      FCURV=(2.*DTI(1)**2/((DCO-DTO(1))**2+(DCI+DTO(1))**2))
     1**0.05
      CUV(NC)=0.0210*FCURV/DTI(NC)
      CUL(NC)=0.0155*FCURV/DTI(NC)
      CEV(NC)=0.184*FCURV
      AFLS(NC1)=AFLS(NC)
   15 IF(KBNDRY.EQ.0) GO TO 28
C        INITIAL CONDITIONS
      READ(5,1)WDS,WDG,TIM
      DO 16 J=1,NC1
      K=J+1
      M=NC1+1-J
      READ(5,2)TG(M),TTO(J),TTC(J),TTI(J),TS(J),PS(K),VS(J),
     1HS(J),US(J)
    2 FORMAT(10F8.0)
      IF(TG(M).NE.0.)GO TO 16
      J1=J-1
      M1=NC1+1-J1
      DO 25 I=J,NC1
      TG(I)=TG(M1)
      TTO(I)=TTO(J1)
      TTC(I)=TTC(J1)
      TTI(I)=TTI(J1)
      TS(I)=TS(J1)
```

```
      PS(I+1)=PS(J)
      VS(I)=VS(J1)
      HS(I)=HS(J1)
25    US(I)=US(J1)*AFLS(J1)/AFLS(I-1)
      TG(1)=TG(2)
      GO TO 29
16    CONTINUE
29    PS(1)=PS(2)
      TSECON=TS(1)
      IF(WDS.EQ.0.) WDS=US(1)*AFLS(1)/VS(1)
28    WRITE(6,7)WDS,WDG
7     FORMAT(1HO, '    WDS      WDG'/
     12F8.1/)
      DO 30 J=1,NC1
      X(J)=0.
      REW(J)=0.5
      DVHP(J)=0.
      DVPH(J)=0.
      DVHPB(J)=0.001
      DVPHB(J)=0.001
      CALL GAST(TG(J),ARWG,HGAD,HG(J),C,V,P,2)
      YG(J)=0.
30    YS(J)=0.
      YV=1.
      YL=1.
      VV=0.
      VL=0.
      FV=0.
      FL=0.
      KCH=1
      NCH=0
      RCH=0.
```

```
      CRCH=5.
      NSTEP=0.
      DTIM=0.
      TP=TIM
C        UPDATE
 70   DO 60 J=1,NC1
      USN(J)=US(J)
      PSN(J)=PS(J)
      HSN(J)=HS(J)
      TSN(J)=TS(J)
      VSN(J)=VS(J)
      XN(J)=X(J)
      DVHPN(J)=DVHP(J)
      DVPHN(J)=DVPH(J)
      TTON(J)=TTO(J)
      TTCN(J)=TTC(J)
      TTIN(J)=TTI(J)
      HGN(J)=HG(J)
 60   TGN(J)=TG(J)
      PSN(NC2)=PS(NC2)
      WDGN=WDG
      NSTEP=NSTEP+1
C        BOUNDARY CONDITIONS
      CALL CONTRL
      PS(NC2)=0.75*PSN(NC2)+0.25*PS(NC2)
C         GAS
 50   ARWG=ARAD/WDG
      CALL GAST(TG(1),ARWG,HGAD,HG(1),C,V,P,1)
      QSCC=(WDG*(HGAD-HG(1))-0.50*ACCLOS*(TG(1)-TAM))/ARAD
      YRAD=QSCC/(TG(1)-TS(NC1))
      DO 21 KREP=1,2
      DO 22 N=2,NC1
```

```
      M=N-1
      J=NC1+1-M
      I=J-1
      YG(I)=0.
      IF(XT(I).LT.0.) HG(N)=HG(1)
      IF(XT(I).LT.0.) TG(N)=TG(1)
      TGB=(TGN(M)+TG(M)+TGN(N)+TG(N))/4.
      IF(XT(I).LT.0.) GO TO 62
      QLOSS=0.50*ALOSS(I)*(TGB-TAM)
      CALL GAST(TGB,ARWG,HGAD,H,CPG,VISG,PRG23,4)
      GG=WDG/AFLG(I)
      REG=GG*DHYD(I)/VISG
      YG(I)=CUG(I)*GG*CPG/(PRG23*REG**0.40)
      DTMN=TGB-0.5*(TTO(I)+TTON(I))
      QC=YG(I)*AHT(I)*DTMN
      HG(N)=HG(M)+HGN(M)-HGN(N)-4.*(QC+QLOSS)/(WDG+WDGN)
      HG(N)=0.50*(HG(N)+HGN(N))
      CALL GAST(TG(N),ARWG,HGAD,HG(N),C,V,P,3)
C          TUBE
   62 TSB=(TS(I)+TSN(I)+TS(J)+TSN(J))/4.
      CTA=CTAO(I)*DTIM
      CTD=1.+2.*CTA*(1.+CT1(I)*YG(I))
      CTE=1.+2.*CTA
      CTF=1.+2.*CTA*(1.+CT4(I)*YS(I))
      CTG=TTON(I)+2.*CTA*CT1(I)*(YG(I)*TGB+FRAD(I)*QSCC)
      CTH=TTIN(I)+2.*CTA*CT4(I)*YS(I)*TSB
      CTW=CTA*CT2(I)
      CTZ=CTA*CT3(I)
      DET=CTD*(CTE*CTF-2.*CTA*CTZ)-2.*CTA*CTW*CTF
      TTO(I)=(2.*CTA*CTZ*(CTH-CTG)+CTF*(CTG*CTE+2.*CTA*
     1TTCN(I)))/DET
      TTC(I)=(CTD*(CTZ*CTH+CTF*TTCN(I))+CTW*CTG*CTF)/DET
```

```
      TTI(I)=(CTD*(CTH*CTE+2.*CTA*TTCN(I))+2.*CTA*CTW*
     1(CTG-CTH))/DET
  22  CONTINUE
C          STEAM
  46  DO 20 J=2,NC1
      I=J-1
      K=J+1
      M=NC1+1-J
      N=M+1
      USB=((US(I)+USN(I))*ARS(J)+US(J)+USN(J))/4.
      PSB=(PS(J)+PSN(J)+PS(K)+PSN(K))/4.
      TSB=(TS(I)+TSN(I)+TS(J)+TSN(J))/4.
      VSB=(VS(I)+VSN(I)+VS(J)+VSN(J))/4.
      XB=(X(I)+XN(I)+X(J)+XN(J))/4.
      GS=DABS(USB/VSB*3600.)
      GS2=USB*DABS(USB)/(VSB*VSB)
      CALL STEAMT(TSI,PSB,VVB,HVB,VIS,COND,PR,4)
      IF(XB.EQ.0.) GO TO 43
C          VAPOR
  61  CALL STEAMT(TSB,PSB,V,H,VISV,CONDV,PRV,8)
      REV=GS*DTI(I)/VISV
      YV=CUV(I)* PRV**0.6* REV**0.85*CONDV
      YS(I)=YV
      FV=CFV(I)/ REV**0.15
      IF(XB.EQ.1) VVB=VSB
      DPV=CDPV(I)*FV*GS2*VVB
      DPS=DPV
      IF(XB  .EQ.1.) GO TO 44
C          LIQUID
  43  CALL STEAMT(TSB,PSB,V,H,VISL,CONDL,PRL,7)
      REL=GS*DTI(I)/VISL
      YL=CUL(I)* PRL**0.5* REL**0.88*CONDL
```

```
      YS(I)=YL
      FL=CFV(I)/ REL**0.15
      CALL STEAMT(TSI,PSB,VLB,HLB,VIS,COND,PF,3)
      IF(XB.EQ.0.) VLB=VSB
      DPL=CDPV(I)*FL*GS2*VLB
      DPS=DPL
      IF(XB.EQ.0) GO TO 44
C        TWO PHASE
      F2PH=1.5-0.5*DCOS(2.*PI*XB)
      YS(I)=(XB*YV+(1.-XB)*YL)*F2PH
      DPS=(XB  *DPV+(1.-XB  )*DPL)*F2PH
C         TOTAL STEAM
 44   DTMN=(TTI(I)+TTIN(I))/2.-TSB
      QV=YS(I)*DTMN/(900.*DTI(I))
      DPSX=DPS/ZT(I)*(-144.)
      VSBW(I)=VSB
      USBW(I)=USB
      QVW(I)=QV
      DPSXW(I)=DPSX
C        TRITSI COEF
      DTX=DTIM/ZT(I)
      CM=1.-DTX*USB
      CP=1.+DTX*USB
      ATRI(1,J)=DTX*VSB*ARS(J)
      BTRI(1,J)=-DTX*VSB
      BTRI(2,J)=DVPHB(J)*CM
      CTRI(2,J)=DVPHB(J)*CP
      ATRI(3,J)=DVHPB(J)*CM
      BTRI(3,J)=DVHPB(J)*CP
      DTRI(1,J)=  DTX*VSB*(USN(J)-USN(I)*ARS(J))+
     1DVPHB(J)*(CP*PSN(J)+CM*PSN(K))+DVHPB(J)*(CP*HSN(I)+
     2CM*HSN(J))
```

```
      ATRI(4,J)=CM*ARS(J)
      BTRI(4,J)=CP
      BTRI(5,J)=-DTX*VSB*GC*144.
      CTRI(5,J)=DTX*VSB*GC*144.
      DTRI(2,J)=CP*USN(I)*ARS(J)+CM*USN(J)-DTX*VSB*(PSN(K)-
     1PSN(J))*GC*144.+2.*DTIM*VSB*DPSX*GC
      ATRI(7,J)=CM*USB/CGJ*ARS(J)
      BTRI(7,J)=CP*USB/CGJ
      BTRI(8,J)=-VSB/CJ*144.
      CTRI(8,J)=-VSB/CJ*144.
      ATRI(9,J)=CM
      BTRI(9,J)=CP
      DTRI(3,J)=CP*HSN(I)+CM*HSN(J)+USB*(CP*USN(I)*ARS(J)+
     1CM*USN(J))/CGJ-VSB*(PSN(K)+PSN(J))*144./CJ+2.*DTIM*
     2VSB*(GV-USB*DPSX/CJ)
      IF(J.NE.2) GO TO 31
      DTRI(1,J)=DTRI(1,J)-ATRI(1,J)*US(1)-ATRI(3,J)*HS(1)
      DTRI(2,J)=DTRI(2,J)-ATRI(4,J)*US(1)
      DTRI(3,J)=DTRI(3,J)-ATRI(7,J)*US(1)-ATRI(9,J)*HS(1)
      ATRI(1,J)=0.
      ATRI(3,J)=0.
      ATRI(4,J)=0.
      ATRI(7,J)=0.
      ATRI(9,J)=0.
   31 IF(J.NE.NC1) GO TO 20
      DTRI(1,J)=DTRI(1,J)-CTRI(2,J)*PS(NC2)
      DTRI(2,J)=DTRI(2,J)-CTRI(5,J)*PS(NC2)
      DTRI(3,J)=DTRI(3,J)-CTRI(8,J)*PS(NC2)
      CTRI(2,J)=0.
      CTRI(5,J)=0.
      CTRI(8,J)=0.
   20 CONTINUE
```

```
      CALL TRITRI
C        NEW X,TS,VS
      DO 99 J=1,NC1
      K=J+1
      US(J)=0.5*(US(J)+USN(J))
      PS(K)=0.5*(PS(K)+PSN(K))
      I=J-1
      IF(J.EQ.1) I=1
      REW(J)=0.5
      X(J)=1.
      CALL STEAMT(TSAT,PS(K),VV,HV,VIS,COND,PR,4)
      IF(HS(J).GT.HV) GO TO 91
      X(J)=0.
      CALL STEAMT(TSAT,PSAT,VL,HL,VIS,COND,PR,3)
      IF(HS(J).LT.HL) GO TO 92
      TS(J)=TSAT
      X(J)=(HS(J)-HL)/(HV-HL)
      VS(J)=VL+X(J)*(VV-VL)
      DPD=-10.
      PS1=PS(K)+DPD
      CALL STEAMT(TS1,PS1,VV1,HV1,VIS,COND,PR,4)
      CALL STEAMT(TS1,PS1,VL1,HL1,VIS,COND,PR,3)
      DVHP(J)=(VV-VL)/(HV-HL)
      DVPH(J)=(X(J)*(VV1-VV)+(1.-X(J))*(VL1-VL)-
     1DVHP(J)*(X(J)*(HV1-HV)+(1.-X(J))*(HL1-HL)))/DPD
      HSBI=0.5*(HS(I)+HSN(I))
      HSBJ=0.5*(HS(J)+HSN(J))
      HSMX=DMAX1(HSBI,HSBJ)
      HSMN=DMIN1(HSBI,HSBJ)
      IF(HL.GT.HSMX.OR.HL.LT.HSMN) GO TO 90
      REW(J)=(HSMX-HL)/(HSMX-HSMN)
      GO TO 90
```

```
91    DTD=10.
      TS2=TSN(J)+DTD
      CALL STEAMT(TSN(J),PS(K),VS1,HS1,VIS,COND,PR,6)
      CALL STEAMT(TS2,PS(K),VS2,HS2,VIS,COND,PR,6)
      TS(J)=TSN(J)+(HS (J)-HS1)/(HS2-HS1)*DTD
      IF(J.EQ.1) TS(1)=TSECON
      CALL STEAMT(TS(J),PS(K),VS(J),HS1,VIS,COND,PR,6)
      DPD=-10.
      PS1=PS(K)+DPD
      TS2=TS(J)+10.
      CALL STEAMT(TS(J),PS(K),VSI,HSI,VIS,COND,PR,6)
      CALL STEAMT(TS2,PS(K),VV2,HV2,VIS,COND,PR,6)
      CALL STEAMT(TS(J),PS1,VV1,HV1,VIS,COND,PR,6)
      DVHP(J)=(VV2-VSI)/(HV2-HSI)
      DVPH(J)=(VV1-VSI-DVHP(J)*(HV1-HSI))/DPD
      IF(J.NE.1) GO TO 90
      HS(1)=HS1
      US(1)=WDS*VS(1)/(3600.*AFLS(1))
      GO TO 90
92    TS(J)=TSAT-(HL-HS(J))/1.035
      IF(J.EQ.1) TS(1)=TSECON
      CALL STEAMT(TS(J),PSAT,VSAT,HS1,VIS,COND,PR,2)
      CALL STEAMT(TS(J),PSAT,VSAT,HS1,VIS,COND,PR,3)
      VS(J)=VSAT-(5.0D-8+5.2D-10*(TS(J)-210.))*(PS(K)-PSAT)
      DVHP(J)=6.55D-6+5.3D-8*(TS(J)-210.)
      DVPH(J)=-6.5D-8-6.4D-10*(TS(J)-210.)
      IF(J.NE.1) GO TO 90
      HS(1)=HS1+0.00212*PS(2)
      US(1)=WDS*VS(1)/(3600.*AFLS(1))
90    DVHPB(J)=0.5*(REW(J)*(DVHP(J)+DVHPN(J))+
     1(1.-REW(J))*(DVHP(I)+DVHPN(I)))
      DVPHB(J)=0.5*(REW(J)*(DVPH(J)+DVPHN(J))+
```

```
     1(1.-REW(J))*(DVPH(I)+DVPHN(I)))
      VSD(J)=0.5*((VS(I)+VSN(I))+DVHPB(J)*(HS(J)+HSN(J)-
     1HS (I)-HSN(I))+DVPHB(J)*(PS(K)+PSN(K)-PS(J)-PSN(J)))
      VT=VS(J)
      VS(J)=0.5*(VSD(J)+VSN(J))
 20   VSD(J)=VT
 21   CONTINUE
      DO 99 J=1,NC1
 99   RCH=RCH+DABS(VS(J)/VSN(J)-1.)+DABS(HS(J)/HSN(J)-1.)
      RCH=RCH/ENCH
C        PRINTOUT
      IF(TIM.LT.TP-1.D-6) GO TO 23
      WRITE(6,4) TIM,DTIM,RCH ,NSTEP
 4    FORMAT(//2F9.4,F10.6,I8)
      DO 95 J=1,NC1
      I=J-1
      M=NC1+1-J
      QVWW=0.
      VSER=VSD(J)/VS(J)-1.
      IF(J.EQ.1) GO TO 95
C        CONSERVATION TEST PRINTOUT
      DT=2.*DTIM+1.D-70
      DX=2.*ZT(I)
      RI=1./VS(I)
      RIN=1./VSN(I)
      RJ=1./VS(J)
      RJN=1./VSN(J)
      UI=US(I)*ARS(J)
      UIN=USN(I)*ARS(J)
      UJ=US(J)
      UJN=USN(J)
      RUI=RI*UI
```

```
      RUIN=RIN*UIN
      RUJ=RJ*UJ
      RUJN=RJN*UJN
      PJ=PS(J)*144.
      PJN=PSN(J)*144.
      PK=PS(J+1)*144.
      PKN=PSN(J+1)*144.
      REI=RI*(HS(I)+UI*UI/CGJ2)-PJ/CJ
      REIN=RIN*(HSN(I)+UIN*UIN/CGJ2)-PJN/CJ
      REJ=RJ*(HS(J)+UJ*UJ/CGJ2)-PK/CJ
      REJN=RJN*(HSN(J)+UJN*UJN/CGJ2)-PKN/CJ
      DRDT=(RI+RJ-RIN-RJN)*AFLS(I)*ZT(I)*3600./DT
      WDSI=(RUI+RUIN)*AFLS(I)*1800.
      WDSJ=(RUJ+RUJN)*AFLS(I)*1800.
      BAL1=(WDSI-WDSJ-DRDT)/WDSJ
      DPS=-DPSXW(I)*ZT(I)/144.
      DRUDT=(RUI+RUJ-RUIN-RUJN)/(DT*GC*DPSXW(I))
      DRU2DX=(RUJ*UJ+RUJN*UJN-RUI*UI-RUIN*UIN)/(DX*GC*
     1DPSXW(I))
      DPDX=(PK+PKN-PJ-PJN)/(DX*DPSXW(I))
      BAL2=DRUDT+DRU2DX+DPDX-1.
      QV=(WDG*(HG(M)-HG(M+1))+FRAD(I)*QSCC*AHT(I))/(AFLS(I)*
     1ZT(I)*3600.)
      DREDT=(REI+REJ-REIN-REJN)/(DT*QV     )
      DREUDX=(REJ*UJ+REJN*UJN-REI*UI-REIN*UIN)/(DX*QV     )
      DPUDX=(PK*UJ+PKN*UJN-PJ*UI-PJN*UIN)/(DX*CJ*QV     )
      DPEUDX=DPSXW(I)*(UI+UIN+UJ+UJN)/(4.*CJ*QV)
      QVV=QVW(I)/QV
      BAL3=DREDT+DREUDX+DPUDX+DPEUDX-QVV
      QVWW=QVW(I)
   95 WRITE(6,5)J,TG(M),TTO(J),TTC(J),TTI(J),TS(J),PS(J+1),
     1X(J),VS(J),HS(J),US(J),WDSJ,BAL1,BAL2,QVWW,BAL3,VSER
```

```
 5     FORMAT(I3,6F8.1,2F8.4,F8.1,F8.2,F8.1,F8.4,F8.4,
     1F8.4,F8.2,2F8.4)
       ITP=(TIM+DTIMMN)/DTP+1.
       ATP=ITP
       TP=ATP*DTP
C         STEP SIZE
 23    CONTINUE
       DTIM=DTIM/(0.90+ CRCH*RCH)+DTIMMN
       RCH=0.
       IF(TIM+DTIM.GT.TP) GO TO 93
       ITIM=(TP-TIM+DTIMMN )/DTIM+1.
       DTIM=ITIM
       DTIM=(TP-TIM)/DTIM
       GO TO 37
 93    IF(DABS(TP-TIM).GT.DTIMMN) GO TO 94
       ITIM=(DTP+DTIMMN)/DTIM+1.
       DTIM=ITIM
       DTIM=DTP/DTIM
       GO TO 37
 94    DTIM=TP-TIM
       GO TO 37
 37    TIM=TIM+DTIM
       IF(TIM.LT.TSTOP) GO TO 70
       STOP
       END
```

```
      SUBROUTINE TRITRI
      IMPLICIT REAL*8(A-H,O-Z)
      COMMON/TRI1/U(28),V(28),W(28),A(9,27),B(9,27),C(9,27),
     1D(3,27),N
      DIMENSION   EL(9,25),GAM(3,25)
      N1=N+1
      DO 10 I=2,N1
      K=I-1
      IF(I.EQ.2) GO TO 11
      BET1=B(1,I)
      BET2=B(2,I)-A(1,I)*EL(2,K)-A(3,I)*EL(8,K)
      BET3=B(3,I)
      BET4=B(4,I)
      BET5=B(5,I)-A(4,I)*EL(2,K)
      BET7=B(7,I)
      BET8=B(8,I)-A(7,I)*EL(2,K)-A(9,I)*EL(8,K)
      BET9=B(9,I)
      DEL1=D(1,I)-A(1,I)*GAM(1,K)-A(3,I)*GAM(3,K)
      DEL2=D(2,I)-A(4,I)*GAM(1,K)
      DEL3=D(3,I)-A(7,I)*GAM(1,K)-A(9,I)*GAM(3,K)
      GO TO 12
11    BET1=B(1,I)
      BET2=B(2,I)
      BET3=B(3,I)
      BET4=B(4,I)
      BET5=B(5,I)
      BET7=B(7,I)
      BET8=B(8,I)
      BET9=B(9,I)
      DEL1=D(1,I)
      DEL2=D(2,I)
      DEL3=D(3,I)
```

```
12    THE1=BET5*BET9
      THE2=          -BET4*BET9
      THE3=BET4*BET8-BET5*BET7
      THE4=BET3*BET8-BET2*BET9
      THE5=BET1*BET9-BET3*BET7
      THE6=BET2*BET7-BET1*BET8
      THE7=          -BET3*BET5
      THE8=BET3*BET4
      THE9=BET1*BET5-BET2*BET4
      EM=THE1*BET1+THE2*BET2+THE3*BET3
      EL(2,I)=(THE1*C(2,I)+THE4*C(5,I)+THE7*C(8,I))/EM
      EL(5,I)=(THE2*C(2,I)+THE5*C(5,I)+THE8*C(8,I))/EM
      EL(8,I)=(THE3*C(2,I)+THE6*C(5,I)+THE9*C(8,I))/EM
      GAM(1,I)=(THE1*DEL1+THE4*DEL2+THE7*DEL3)/EM
      GAM(2,I)=(THE2*DEL1+THE5*DEL2+THE8*DEL3)/EM
      GAM(3,I)=(THE3*DEL1+THE6*DEL2+THE9*DEL3)/EM
10    CONTINUE
      U(N1)=GAM(1,N1)
      V(N1)=GAM(2,N1)
      W(N1)=GAM(3,N1)
      DO 30 I=2,N
      J=N1+1-I
      J1=J+1
      U(J)=GAM(1,J)                -EL(2,J)*V(J1)
      V(J)=GAM(2,J)                -EL(5,J)*V(J1)
30    W(J)=GAM(3,J)                -EL(8,J)*V(J1)
      RETURN
      END
```

```
      SUBROUTINE GAST(TG,ARWG,HGAD,HG,CPG,VIS,PRG23,M)
      IMPLICIT REAL*8(A-H,O-Z)
      GO TO (1,2,3,4),M
    1 TG=(HGAD-34.+6900.*ARWG)/(0.336+6.2*ARWG)
    2 HG   =112.9033+(.2652727+1.390926E-5*TG)*TG
      RETURN
    3 TG  =-414.3591+(3.769359-.0004481329*HG)*HG
      RETURN
    4 CPG=0.2550812+( .4023570E-4+(- .9408869E-9-
     1 .8431375E-12*TG)*TG)*TG
      VIS=0.03632385+( .5439683E-4+(- .8065211E-8+
     1.5337830E-12*TG)*TG)*TG
      PRG23=0.7882808+( .2263911E-3+(- .1580168E-6+(
     1.5023598E-10-.5769971E-14*TG)*TG)*TG)*TG
      RETURN
      END
```

```
      SUBROUTINE STEAMT(TF,PA,V,H,VIS,CON,PR,J)
      IMPLICIT REAL*8(A-H,O-Z)
      GOTO(1,2,3,1,2,6,7,8),J
C          TSAT=F(P)
 1    IF(PA.GE.450.) GO TO 21
      A=DLOG(10.*PA)
      TF=35.15789+A*(24.59259+A*(2.118207-A*.3414474+A*(
     1.1574164*A+A*(-.03132959*A+A*(.003865828*A+A*(-
     2.0002490178*A+A*(A*.6840156E-5)))))))
      GO TO 22
 21   A=DLOG(PA)
      TF=11545.16+A*(-3386.018+A*(2477.766-363.4427*A+
     1A*(26.69098*A+A*(-.7807381*A))))
 22   IF(J.EQ.4) GO TO 6
      RETURN
C          PSAT=F(T)
 2    TK=.5555556*(TF-32.)+273.16
      A=647.27-TK
      IF(TF.GT.200.) GO TO 31
      P=218.167/(10.**((A/TK)*((3.243781+.00586826*A+
     1.1170E-7*A**3)/(1.+.002187846*A))))
      GO TO 32
 31   P=218.167/(10.**((A/TK)*((3.346313+.0414113*A+
     1.7515484E-8*A**3+.65644E-10*A**4)/(1.+.01379448*A))))
 32   PA=P*14.696
      IF(J.EQ.5) GO TO 6
      RETURN
C          SAT LIQ V,H,S=F(T)
 3    X=705.398-TF
      IF(X.GT.0.) GO TO 34
      V=0.
      RETURN
```

```
 34   V=(.05121915-4.150065E-3*X**.3333333-1.070903E-5*X+
     1X**4*.8750628E-15)/(1.+.1103621*X**.3333333-
     22.192368E-3*X)
      IF(TF.GT.360.) GO TO 36
      H=-32.17911+1.008808*TF-1.1517E-4*TF**2+4.855384E-7*
     1TF**3-7.361878E-10*TF**4+9.635032E-13*TF**5
      RETURN
 36   H=-904.1171+10.6738*TF-.04275384*TF**2+9.41244E-5*
     1TF**3-1.031536E-7*TF**4+4.560246E-11*TF**5
      RETURN
C          SUPERHEAT V,H,S=F(T,P) AND SAT VAP V,H,S=F(P)
  6   TC=0.5555556*(TF-32.)
      P=PA/14.696
      A=1./(TC+273.16)
      B=2641.62*10.**(80870.*A**2)
      C=80870.*DLOG(10.D0)*A**2
      D=B*(1.+2.*C)
      E=82.546-162460.*A
      F=.21828-126970.*A**2
      G=.0003635-.6768E-7*(1000.*A)**24
      Q=1.89-A*B
      R=P**2/2.
      U=(A*P)**4/4.
      IF(U.GT.1.E-7) GO TO 10
      W=0.
      X=0.
      GO TO 11
 10   W=(A*P)**13/13.
      X=(A*P)**12
 11   G1=Q**2*A**2*(3.*E-162460.*A)-F*A**3*2.*Q*D
      G2=Q**4/A*(4.*F-253940.*A**2)-F*4.*Q**3*D
      G3=-Q**12*C/A*(13.*G-.162432E-5*(1000.*A)**24)+G*13.*
```

```
     10**12*D
      V=(4.55504/(P*A)+Q+Q**2*A**2*E*P+Q**4*(A*P)**3*F-Q**12
     1*Q*X*G)*.0160185
      H=((P*(1.89-2.*A*B*(1.+C))+G1*R+G2*U+G3*W)*.101295+
     11.472/A+.00037783/A**2-47.8365*DLOG(A)+1803.71)*.43
      RETURN
C          LIQUID PROPERTIES
  7   VIS=1./(.00833*TF -.225)
      CON=0.322+(.00554-9.835E-7*TF)*TF
      PR  =10.84+(-.09349+(.0003388+(-.5523E-6+.3366E-9*TF)
     1*TF)*TF)*TF
      RETURN
C          VAPOR PROPERTIES
  8   VIS=0.122-(5.54E-5-1.96E-9*PA )*(1885.-TF )
      CON=-0.00840+2.036E-6*PA+4.652E-5*TF+3.817/(TF-0.285*PA)
      PR=0.523-0.00005079*PA+0.0001585*TF+214./(TF-0.246*PA)
      RETURN
      END
```

```
      SUBROUTINE CONTRL
      IMPLICIT REAL*8(A-H,O-Z)
      COMMON /TRI1  / US(28),PS(28),HS(28),ATRI(9,27),
     1BTRI(9,27),CTRI(9,27),DTRI(3,27),NC
      COMMON /CNTRL1/TIM,DTIM,TP,DTP,TSTOP,WDS,WDG,AVAT,
     1VS(27),X(27),TS(27),NSTEP,KCH
      GO TO (1,2,3      ),KCH
    1 DTP=1.0
      TSTOP=320.+1.D-6
      NC1=NC+1
      AVAT=0.06865
      PI2=3.141592653589*2.
      KCH=2
    2 CONTINUE
      IF(TIM.LT.20.0+1.D-6) GO TO 4
      DTIM=0.
      KCH=3
    3 CONTINUE
      WDS=300.+18.*DSIN(PI2*(TIM-20.)/60.)
    4 CONTINUE
      PS(NC+2)=(US(NC1)/(45.5*AVAT))**2/VS(NC1)
      RETURN
      END
```

The vita has been removed from the scanned document

TRANSIENTS IN A MONOTUBE BOILER

--A DIGITAL SIMULATION

by

Arthur Wilfred Gardiner

(ABSTRACT)

A steam generating unit consisting of a single tube heated by combustion gases has been modeled mathematically with emphasis on simulating non-steady behavior. The resulting digital computer program is particularly suited to predicting the response of automotive boilers to changes in operating conditions.

The heart of the model is the set of conservation laws for mass, momentum and energy of the steam. These are augmented with empirical relations for heat transfer and pressure drop plus steam table data. Allowance is also made for gas convection and radiation, heat loss to ambient, and energy storage in the tube wall. The resulting set of three partial differential equations in four unknowns is solved by removing specific volume derivatives from the set through substitution of steam table data in differential form. The differential equations are put in finite difference form which yields a set of quasi-linear algebraic relations which are solved on a digital computer. The program's predictions of non-steady performance have been qualitatively compared with experimental results found in the literature. A 12-in.

diameter test boiler has been constructed and preliminary steady-state data from it are compared with the simulation.